

# AGNs with composite spectra <sup>\*</sup>

## II. Additional data

A. C. Gonçalves, M.-P. Véron-Cetty and P. Véron

Observatoire de Haute-Provence (CNRS), F-04870 Saint Michel l'Observatoire, France

Received 11 August 1998 / Accepted 17 November 1998

**Abstract.** In a previous paper (Véron et al. 1997) we presented medium resolution (3.4 Å FWHM) spectroscopic observations of 15 “transition objects”, selected for having an ambiguous location in the Veilleux & Osterbrock (1987) diagnostic diagrams, and showed that most of them were in fact “composite”, this being due to the simultaneous presence on the slit of both a Seyfert or Liner nucleus and a H II region. Here, we report new spectroscopic observations of 53 emission-line galaxies with a “transition” spectrum, bringing up to 61 the total number of observed objects in an unbiased sample of 88 “transition objects”. Almost all of the observed galaxies have a “composite” nature, confirming the finding that true “transition” spectra may not exist at all.

By eliminating “composite objects” from the diagnostic diagrams, a clear separation between the different classes of nuclear emission-line regions (Seyfert 2s, Liners and H II regions) becomes apparent; by restricting the volume occupied by the different line-emitting regions in the 3-dimensional diagnostic diagrams, we are also restricting the range of possible physical parameters in these regions. There seems to be no continuity between Seyfert 2s and Liners, the two classes occupying distinct volumes in the 3-dimensional space defined by  $\lambda 5007/H\beta$ ,  $\lambda 6583/H\alpha$ , and  $\lambda 6300/H\alpha$ .

**Key words:** galaxies: active – galaxies: nuclei

### 1. Introduction

The use of the Baldwin et al. (1981) or Veilleux & Osterbrock (1987) diagnostic diagrams generally yields an immediate classification of the nuclear emission-line clouds; “transition objects” exist however, which cannot be classified unambiguously from their line ratios (Heckman et al. 1983; Keel 1984; Veilleux

& Osterbrock 1987; Ho et al. 1993a). When observed with sufficient spectral resolution, such objects show different profiles for the permitted and forbidden lines (Heckman et al. 1981; Busko & Steiner 1990; Véron et al. 1981a,b; Véron-Cetty & Véron 1985, 1986b).

In a previous paper (Véron et al. 1997, hereafter Paper I), we presented high-dispersion (66 Å mm<sup>-1</sup>) spectroscopic observations of 15 “transition objects” selected for having an ambiguous location on the Veilleux & Osterbrock (1987) diagnostic diagrams, and showed that most of them are in fact “composite”. This was done by modelling the H $\alpha$ , [N II] $\lambda\lambda$  6548, 6583 and/or H $\beta$ , [O III] $\lambda\lambda$  4959, 5007 emission lines with Gaussian profiles, allowing for the contribution of several components; best fits showed these components to have different line strengths and widths, as the result of the lines being produced in regions that are kinematically and spatially distinct, usually a Seyfert 2 or Liner cloud and a H II region.

We have found in the literature 88 emission-line galaxies located north of  $\delta \sim -20^\circ$ , with  $z < 0.100$  and  $B < 17.0$ , for which the published line ratios gave indication of a “transition” spectrum, constituting an unbiased sample of such objects. Here we report results for 53 of these galaxies, including seven already observed in Paper I, bringing up to 61 the total number of observed objects, or 70% of our unbiased sample of galaxies with a “transition” spectrum.

### 2. Observations and data analysis

#### 2.1. Observations

The 53 observed galaxies suspected to have a “transition” spectrum are listed in Table 1 with the various names under which they are known, and in Table 2 with the published line intensity ratios  $\lambda 5007/H\beta$ ,  $\lambda 6300/H\alpha$  and  $\lambda 6583/H\alpha$ . Table 3 gives their optical positions measured on the Digitized Sky Survey<sup>1</sup> (Véron-Cetty & Véron 1996).

Spectroscopic observations were carried out during several observing runs in May, June and July 1996 and January, March, October and November 1997 with the spectrograph CARELEC (Lemaître et al. 1989) attached to the Cassegrain focus of the

<sup>1</sup> The Digitized Sky Survey was produced at the Space Telescope Science Institute (STScI) under U.S. Government grant NAG W-2166.

Send offprint requests to: A. C. Gonçalves, anabela@obs-hp.fr

<sup>\*</sup> Based on observations collected at the Observatoire de Haute-Provence (CNRS), France, and *Hubble Space Telescope (HST)* data obtained from the Space Telescope European Coordinating Facility (ST-ECF) archive. Tables 5 and 6 are also available in electronic form at the CDS via anonymous ftp to cdsarc.u-strasbg.fr (130.79.128.5) or via <http://cdsweb.u-strasbg.fr/Abstract.html>.

Observatoire de Haute-Provence (OHP) 1.93 m telescope. The detector was a  $512 \times 512$  pixels,  $27 \times 27 \mu\text{m}$  Tektronic CCD. We used a  $600 \text{ l mm}^{-1}$  grating resulting in a dispersion of  $66 \text{ \AA mm}^{-1}$ ; the spectral range was  $\lambda\lambda 6700\text{--}7600 \text{ \AA}$  in the red (with a Schott GG 435 filter) and  $\lambda\lambda 4860\text{--}5760 \text{ \AA}$  in the blue. In each case, the galaxy nucleus was centered on the slit.

Usually five columns of the CCD ( $\sim 5''$ ) were extracted. The slit width was  $2''.1$ , corresponding to a projected slit width on the detector of  $52 \mu\text{m}$  or 1.9 pixel. The slit position angle was not always the same for the blue and red spectra; as the aperture used is rectangular ( $2''.1 \times 5''$ ), this may introduce some inconsistencies when the line emitting regions are extended. The resolution, as measured on the night sky emission lines, was  $\sim 3.4 \text{ \AA FWHM}$ . The spectra were flux calibrated using the standard stars given in Table 4, taken from Oke (1974), Stone (1977), Oke & Gunn (1983) and Massey et al. (1988). The journal of observations is given in Table 5.

## 2.2. Line profile fitting

Morgan (1958, 1959) has introduced a classification of galaxies based on their nuclear region stellar population. Classes “a” and “af” are dominated by early-type stars. The main absorption features are the Balmer lines, which are usually filled up by emission as these objects invariably contain a H II region. Classes “g”, “gk” and “k” are dominated by a bulge of old population II stars. Intermediate classes “f” and “fg” have, in addition to a population of young stars, a faint bulge of old stars. The old star population have similar spectra in all classes (Bica 1988). AGN activity is exceptional in classes “a” and “af” but frequent in all other classes (Véron & Véron-Cetty 1986); in consequence, the nuclear region of most AGNs contains a population of old stars with many strong absorption lines which can make the line fitting analysis rather difficult, especially for the blue spectra. Therefore, when the absorption blend Mg I b  $\lambda 5175$  was prominent, we subtracted a suitable fraction of the spectrum of the elliptical galaxy NGC 5982, used as a template, to remove the old stellar population contribution. Another elliptical, NGC 4365, was used as a template for the red spectra, while NGC 821 was used for both the red and blue spectra obtained in October and November 1997. All templates were observed with the same spectral resolution as the emission-line galaxies.

Whenever necessary, we have added a  $\text{H}\alpha$  or  $\text{H}\beta$  absorption component; as, usually, the  $\text{H}\alpha$  absorption line is completely filled up by the emission lines, we assumed its intensity to be 1.8 times the intensity of the nearby absorption Ca I  $\lambda 6495$  line (Véron-Cetty & Véron 1986b). Whenever a template and/or absorption component was used in a fit, this is indicated in Table 6 which contains the line fitting analysis results for the 53 observed galaxies.

**Table 4.** Spectrograph settings and standard stars.

Date	$\lambda$ Range ( $\text{\AA}$ )	Standard stars
21 – 22.03.95	6500 – 7400	BD 26°2606
09 – 10.05.96	6700 – 7600	GD 140, BD 26°2606
11 – 13.05.96	4860 – 5760	Feige 98, Kopff 27
08.06.96	4860 – 5760	Feige 66, Kopff 27
09.06.96	6700 – 7600	Feige 66, BD 28°4211
15 – 16.07.96	4675 – 5575	BD 28°4211
23 – 25.07.96	6335 – 7235	BD 28°4211
07.01.97	4720 – 5620	EG 247
10.01.97	6175 – 7075	EG 247
04 – 07.03.97	4825 – 5725	Feige 66
08 – 12.03.97	6310 – 7210	Feige 66
13.03.97	4825 – 5725	Feige 66
31.10.97	6455 – 7365	Feige 24
01 – 02.11.97	4655 – 5560	Feige 24

**Table 1.** Cross-reference names for the galaxies studied in this paper.

NGC	UGC	Zw	MCG	Mark	KUG	IRAS	Misc.
0034	–	–	–02.01.032	938	–	00085–1223	–
–	–	–	–	957	–	00391+4004	5C 3.100
–	–	–	–	–	–	01346–0924	–
–	2456	524.040	06.07.027	1066	–	02568+3637	–
–	–	–	–	–	–	03355+0104	HS 0335+0104
–	–	–	–	–	–	04210+0400	–
–	–	420.015	–	–	–	04507+0358	–
–	–	–	–	–	–	06256+6342	VII Zw 73
–	4229	207.033	–	622	0804+391	08043+3908	–
–	–	–	–	–	–	–	3C 198.0
–	–	–	–	–	0825+248	–	–
–	–	–	–	–	–	09111–1007	–
–	–	238.066	–	–	–	09277+4917	SBS 0927+493
–	5101	289.011	10.14.025	–	–	09320+6134	–
2989	–	–	–03.25.020	–	–	09430–1808	ESO 566–G09
–	–	–	–	–	–	09581+3126	CG 49
3185	5554	123.034	04.24.024	–	–	10148+2156	–
–	5984	155.031	05.26.024	–	–	–	Arp 107A
3504	6118	155.049	05.26.039	–	1100+282	11004+2814	TEX 1100+282
–	–	–	–	–	–	11058–1131	–
3642	6385	291.062	10.16.128	–	–	11194+5920	–
3660	–	–	–01.29.016	1291	–	11210–0823	–
–	–	291.074	10.17.004	–	–	11258+5806	SBS 1125+581
–	–	–	–	–	–	11285+8240 A	–
3758	–	126.110	04.27.073	739	–	11338+2152	–
–	–	–	–	–	–	–	SBS 1136+594
3994	6936	186.074	06.26.059	–	1155+325 A	–	Arp 313
4102	7096	269.036	09.20.094	–	–	12038+5259	–
–	–	–	–	–	–	12474+4345 S	–
–	8621	218.030	07.28.041	–	–	13354+3924	–
5256	8632	246.021	08.25.031	266	–	13362+4832	I Zw 67
–	–	073.074	–	1361	–	13446+1121	–
–	8718	190.055	06.30.085	461	1345+343	–	CG 1190
–	–	162.010	05.33.005	–	–	–	4C 26.42
–	–	–	–	–	–	14063+4905	I Zw 81
–	–	273.023	–	477	1439+537	14390+5343	I Zw 92
–	–	221.050	–	848	–	15163+4255	I Zw 107
–	–	077.080	–	–	–	15184+0834	–
5953	9903	107.008	03.40.005	1512	–	15322+1521	Arp 91
–	–	319.034	11.19.030	–	–	15564+6359	Kaz 49
–	–	–	–	–	–	16129–0753	–
–	–	–	–	–	–	16382–0613	–
–	10675	169.035	05.40.034	700	1701+315	17013+3131	–
–	–	112.010	03.45.003	–	–	17334+2049	–
–	–	142.019	–	–	–	18101+2152	PGC 61548
–	–	341.006	–	–	–	18462+7207	Kaz 214
6764	11407	256.007	08.35.003	–	–	19070+5051	–
–	–	–	–	–	–	22114–1109	–
–	–	452.043	03.57.031	308	2239+199	22395+2000	–
–	–	–	–	522	2257+161	–	–
7465	12317	453.050	03.58.024	313	2259+156	22595+1541	PG 2259+156
–	–	453.062	–	–	–	23024+1916	–
–	–	475.036	04.54.038	–	–	23135+2516	IC 5298

**Table 2.** Published line intensity ratios for the 53 emission-line galaxies studied in this paper. References: (1) Aguero et al. (1995), (2) Anton (1993), (3) Augarde et al. (1994), (4) Boller et al. (1994), (5) Cohen & Osterbrock (1981), (6) de Grijp et al. (1992), (7) Delgado & Perez (1996), (8) Duc et al. (1997), (9) Fruscione & Griffiths (1991), (10) Goodrich & Osterbrock (1983), (11) Hill et al. (1988), (12) Ho et al. (1997a), (13) Keel et al. (1985), (14) Kim et al. (1995), (15) Klaas & Elsasser (1991), (16) Kollatschny et al. (1983), (17) Koratkar et al. (1995), (18) Koski (1978), (19) Martel & Osterbrock (1994), (20) Netzer et al. (1987), (21) Osterbrock & Pogge (1987), (22) Osterbrock & Martel (1993), (23) Phillips et al. (1983), (24) Rafanelli et al. (1990), (25) Salzer et al. (1995), (26) Shuder & Osterbrock (1981), (27) Ulvestad & Wilson (1983), (28) Veilleux & Osterbrock (1987), (29) Véron et al. (1997), (30) Vogel et al. (1993).

Name	$\frac{\lambda 5007}{H\beta}$	$\frac{\lambda 6300}{H\alpha}$	$\frac{\lambda 6583}{H\alpha}$	Ref.	Name	$\frac{\lambda 5007}{H\beta}$	$\frac{\lambda 6300}{H\alpha}$	$\frac{\lambda 6583}{H\alpha}$	Ref.
Mark 938	3.98	0.09	1.29	(14)	IRAS 12474+4345 S	2.93	–	0.42	(6)
Mark 957	0.63	0.04	0.46	(19)	UGC 8621	5.25	0.081	0.95	(22)
IRAS 01346–0924	2.90	–	0.41	(6)	Mark 266 NE	1.41	0.15	0.66	(22)
Mark 1066	4.35	0.084	0.88	(10)	Mark 266 SW	3.98	0.05	0.50	(22)
IRAS 03355+0104	13.52	0.06	0.18	(30)	Mark 1361	4.93	0.038	0.33	(14)
”	12.41	–	0.58	(6)	Mark 461	–	–	–	–
IRAS 04210+0400	14.2	0.13	0.35	(11)	4C 26.42	0.40	0.22	0.81	(2)
IRAS 04507+0358	11.77	–	0.28	(6)	I Zw 81	3.14	0.066	0.67	(18)
VII Zw 73	3.96	–	0.56	(6)	Mark 477	10.42	0.17	0.36	(26)
Mark 622	6.25	0.064	0.94	(26)	Mark 848 S	1.39	0.070	0.78	(14)
3C 198.0	2.13	0.04	0.35	(5)	IRAS 15184+0834	5.60	–	0.42	(6)
KUG 0825+248	0.84	0.13	0.28	(3)	NGC 5953	3.04	0.10	1.24	(13)
IRAS 09111–1007 E	3.94	0.07	0.74	(8)	”	2.08	0.058	0.78	(14)
Zw 238.066	1.73	0.065	0.82	(14)	”	4.3	0.11	1.38	(7)
UGC 5101	2.86	0.089	1.34	(14)	”	4.98	0.10	1.12	(24)
NGC 2989	2.50	0.037	0.52	(23)	Kaz 49	2.58	0.025	0.56	(4)
CG 49	11.68	–	0.30	(25)	IRAS 16129–0753	2.03	–	0.64	(6)
NGC 3185	3.42	0.045	0.70	(12)	IRAS 16382–0613	6.67	0.09	1.09	(1)
Arp 107A	13.62	0.38	3.00	(13)	Mark 700	0.55	0.11	1.75	(18)
NGC 3504	0.53	0.023	0.59	(12)	MCG 03.45.003	9.74	–	0.42	(6)
IRAS 11058–1131	9.10	0.05	0.38	(29)	PGC 61548	1.44	0.11	0.69	(9)
NGC 3642	1.32	0.08	0.71	(12)	Kaz 214	5.23	–	0.39	(6)
Mark 1291	3.18	–	0.48	(16)	NGC 6764	0.53	0.045	0.68	(18)
IRAS 11285+8240 A	8.25	0.106	0.46	(15)	IRAS 22114–1109	4.22	0.077	0.62	(14)
Mark 739 W	1.14	–	0.43	(20)	Mark 308	4.8	0.05	0.40	(29)
”	1.18	–	0.69	(27)	Mark 522	3.23	0.068	0.93	(29)
SBS 1136+594	12.30	0.11	0.25	(19)	Mark 313	3.52	0.10	0.52	(21)
NGC 3994	0.56	0.19	0.89	(13)	Zw 453.062	1.23	0.12	1.23	(14)
NGC 4102	0.99	0.041	0.92	(12)	IC 5298	4.68	0.05	0.95	(14)

**Table 3.** B1950 optical positions of the observed objects measured on the Digitized Sky Survey. The r.m.s. error is  $0''.6$  in each coordinate; “\*” indicates objects with larger errors due to their location near one edge of the Schmidt plate (Véron-Cetty & Véron 1996). References for finding charts: (1) Andreasian & Alloin (1994), (2) Arp (1966), (3) Bowen et al. (1994), (4) Carballo et al. (1992), (5) de Grijp et al. (1987), (6) Delgado & Perez (1996), (7) Duc et al. (1997), (8) Kazarian (1979), (9) Keel (1996), (10) Markarian & Lipovetski (1971), (11) Markarian & Lipovetski (1973), (12) Markarian & Lipovetski (1974), (13) Markarian et al. (1979a), (14) Markarian et al. (1979b), (15) Markarian & Stepanian (1983), (16) Mazzarella & Boroson (1993), (17) Olsen (1970), (18) Pesch & Sanduleak (1983), (19) Rubin et al. (1975), (20) Sandage & Bedke (1994), (21) Takase & Miyauchi-Isobe (1986), (22) Takase & Miyauchi-Isobe (1990), (23) Vogel et al. (1993), (24) Wyndham (1966).

Name	$\alpha$	$\delta$	Ref.	mag.	Name	$\alpha$	$\delta$	Ref.	mag.
Mark 938	00 08 33.41	− 12 23 06.6	(16)	13.5	IRAS 12474+4345 S	12 47 25.08	43 45 16.6	(5)	15.4
Mark 957	00 39 09.65	40 04 51.6	(3)	15.1	UGC 8621	13 35 28.44	39 24 30.8	–	14.2
IRAS 01346−0924	01 34 37.53	− 09 24 12.9	(5)	15.8	Mark 266 SW	13 36 14.50	48 31 47.4	(16)	13.4
Mark 1066	02 56 49.91	36 37 21.1	(16)	14.0	Mark 266 NE	13 36 14.99	48 31 53.5	(16)	13.4
IRAS 03355+0104	03 35 35.77	01 04 34.0	(23)	14.5	Mark 1361	13 44 36.53	11 21 20.1	(14)	15.3
IRAS 04210+0400	04 21 02.69	04 01 08.2	(5)	16.3	Mark 461	13 45 04.29	34 23 51.9	(9)	14.6
IRAS 04507+0358	04 50 47.50	03 58 48.9	(5)	15.0	4C 26.42	13 46 33.84	26 50 26.3	(17)	15.2
VII Zw 73	06 25 37.78	63 42 42.9	(5)	14.8	I Zw 81	14 06 20.29	49 05 56.1	–	16.5
Mark 622	08 04 21.03	39 08 57.4	(12)	14.1	Mark 477	14 39 02.52	53 43 03.3	(9)	15.0
3C 198.0	08 19 52.43	06 06 45.7	(24)	17.3	Mark 848 S	15 16 19.40	42 55 35.9	(16)	15.0
KUG 0825+248	08 25 29.98	24 48 31.9	(21)	16.0	IRAS 15184+0834	15 18 27.10	08 34 33.9	(5)	13.9
IRAS 09111−1007 E	09 11 13.06	− 10 06 54.6	(7)	16.1	NGC 5953	15 32 13.23	15 21 35.9	(6)	13.1
Zw 238.066	09 27 45.68	49 18 00.4	–	16.5	Kaz 49	15 56 26.70	63 59 00.8	(8)	15.3
UGC 5101	09 32 04.95	61 34 36.5	(9)	15.5	IRAS 16129−0753	16 12 58.38	− 07 53 07.2	(4)	–
NGC 2989	09 43 03.79	− 18 08 35.1	(20)	14.5	IRAS 16382−0613	16 38 11.57	− 06 13 07.6	(4)	14.7
CG 49	09 58 07.76	31 26 44.7	(18)	16.0	Mark 700	17 01 21.49	31 31 37.8	(9)	15.5
NGC 3185	10 14 53.07	21 56 18.8	(20)	12.3	MCG 03.45.003*	17 33 25.27	20 49 37.6	(5)	13.4
Arp 107A	10 49 29.66	30 19 25.1	(2)	14.6	PGC 61548	18 10 07.06	21 52 15.9	–	14.2
NGC 3504	11 00 28.55	28 14 31.6	(20)	12.9	Kaz 214	18 46 15.77	72 07 42.9	(5)	15.5
IRAS 11058−1131	11 05 49.65	− 11 31 56.8	(5)	14.9	NGC 6764	19 07 01.23	50 51 08.5	(19)	13.2
NGC 3642	11 19 25.03	59 20 54.9	(20)	14.1	IRAS 22114−1109	22 11 26.01	− 11 09 21.1	–	–
Mark 1291	11 21 00.13	− 08 23 01.5	(13)	15.5	Mark 308	22 39 30.53	20 00 00.1	(10)	14.6
IRAS 11285+8240 A	11 28 41.22	82 40 16.0	–	15.6	KUG 2239+200 A	22 39 33.13	20 00 38.4	(22)	15.5
Mark 739 W*	11 33 52.49	21 52 22.2	(16)	14.0	Mark 522	22 57 50.44	16 06 50.7	(11)	17.0
SBS 1136+594	11 36 24.27	59 28 31.4	(15)	16.0	Mark 313	22 59 32.07	15 41 44.3	(10)	14.0
NGC 3994*	11 55 02.44	32 33 21.1	(20)	12.9	Zw 453.062	23 02 28.55	19 16 55.2	–	15.1
NGC 4102	12 03 51.33	52 59 21.2	(20)	12.6	IC 5298	23 13 33.13	25 17 01.9	(1)	14.9

**Table 5.** Journal of observations. A:  $66 \text{ \AA mm}^{-1}$ , red; B:  $66 \text{ \AA mm}^{-1}$ , blue. A “\*” indicates objects published in Paper I.

Name	Disp.	Date	Exp. time (min)	PA ( $^{\circ}$ )	Name	Disp.	Date	Exp. time (min)	PA ( $^{\circ}$ )
Mark 938	A	31.10.97	20	90	UGC 8621	A	10.05.96	20	180
	B	01.11.97	20	180		B	11.05.96	20	179
Mark 957	A	10.01.97	20	90	Mark 266 SW	A	10.01.97	20	180
	B	01.11.97	20	270		B	07.03.97	20	215
IRAS 01346–0924*	A	10.01.97	20	90	Mark 266 NE	B	07.03.97	20	215
Mark 1066	A	10.01.97	20	90	Mark 1361*	B	06.03.97	20	180
	B	07.01.97	20	90	Mark 461	A	22.03.95	20	90
IRAS 03355+0104	A	10.01.97	20	90		B	08.06.96	20	89
	B	04.03.97	20	90	4C 26.42	A	09.06.96	20	90
IRAS 04210+0400	A	10.01.97	20	90		B	13.05.96	20	0
	B	07.01.97	20	90	I Zw 81	A	10.05.96	20	180
IRAS 04507+0358	A	10.01.97	20	90		B	11.05.96	20	84
	B	06.03.97	20	180	Mark 477*	B	11.05.96	20	120
VII Zw 73	A	10.01.97	20	180	Mark 848 S	A	22.06.96	20	171
	B	07.01.97	20	180		B	08.06.96	20	90
Mark 622	A	10.01.97	20	180	IRAS 15184+0834	A	08.03.97	20	270
	B	07.01.97	20	180		B	07.03.97	20	270
3C 198.0	A	12.03.97	20	270	NGC 5953	A	10.05.96	20	180
KUG 0825+248	A	08.03.97	20	220		B	11.05.96	20	180
	B	07.03.97	20	217	Kaz 49	A	22.06.96	20	180
IRAS 09111–1007 E	A	08.03.97	20	258		B	23.06.96	20	180
	B	05.03.97	20	252	IRAS 16129–0753	A	22.06.96	20	180
Zw 238.066	A	08.03.97	20	180		B	15.07.96	20	180
	B	07.01.97	20	90	IRAS 16382–0613	A	09.05.96	20	180
UGC 5101	A	10.03.97	20	270		B	13.05.96	20	0
	B	06.03.97	20	180	Mark 700	A	09.05.96	20	180
NGC 2989	A	09.03.97	20	270		B	07.06.96	20	90
	B	06.03.97	20	180		B	08.06.96	20	90
CG 49	A	10.05.96	20	180	MCG 03.45.003*	B	13.05.96	20	0
	B	01.11.97	20	270	PGC 61548*	A	09.05.96	20	180
NGC 3185	A	08.03.97	20	270		B	13.05.96	20	0
	B	06.03.97	20	180	Kaz 214	A	09.06.96	20	139
Arp 107A	A	09.03.97	20	270		B	13.05.96	20	0
NGC 3504	A	08.03.97	20	270	NGC 6764	A	09.06.96	20	253
	B	07.03.97	20	180		B	08.06.96	20	72
IRAS 11058–1131*	B	06.03.97	20	180	IRAS 22114–1109	A	24.07.96	20	180
NGC 3642	A	08.03.97	20	270		A	25.07.96	20	180
	B	07.03.97	20	180		B	15.07.96	20	180
Mark 1291	A	10.01.97	20	180		B	16.07.96	20	180
	B	06.03.97	20	180	Mark 308*	A	09.06.96	20	44
IRAS 11285+8240 A	A	10.05.96	20	180	Mark 522	A	23.07.96	20	180
Mark 739 W	A	09.01.97	20	90		B	15.07.96	20	180
	B	07.03.97	20	272	Mark 313	A	23.07.96	20	180
SBS 1136+594	A	10.01.97	20	180		B	15.07.96	20	180
	B	05.03.97	20	180	Zw 453.062	A	25.07.96	20	225
NGC 3994	A	08.03.97	20	270		B	01.11.97	20	270
	B	13.03.97	20	180		B	02.11.97	60	270
NGC 4102	A	21.03.95	20	90	IC 5298	A	25.07.96	15	204
	B	04.03.97	15	270		B	02.11.97	60	270
IRAS 12474+4345 S	A	11.03.97	20	345					
	B	13.03.97	20	345					

**Table 6.** Fitting profile analysis results. Col. 1 gives the name of the object, col. 2 the adopted redshift, cols. 4 and 9 the velocities for each set of components measured on the blue and red spectra, respectively, and de-redshifted using the redshift given in col. 2; cols. 5 and 10 the corresponding FWHM, cols. 6, 11 and 12 the intensity ratios  $\lambda 5007/H\beta$ ,  $\lambda 6583/H\alpha$  and  $\lambda 6300/H\alpha$  respectively, and cols. 7 and 13 the fraction of the  $H\beta$  emission flux (respectively  $H\alpha$ ) in each component with respect to the total flux of the line in each object. A “T” in col. 3 (or 8) indicates that the blue (or red) spectrum has been corrected for starlight using a suitable fraction of a template (in the blue, we have used the elliptical galaxy NGC 5982 and in the red, the elliptical galaxy NGC 4365; NGC 821 was used as a template for the objects observed in October and November 1997); in the same columns, an “A” indicates that a  $H\beta$  (or  $H\alpha$ ) absorption component was added to the model. In col. 14 we give the velocity difference between the blue and red systems, and in col. 15 the spectroscopic classification of each component in the model; Gaussian profiles were used throughout, except when indicated by “ $l_z$ ” (Lorentzian profile). Values in parenthesis have been fixed.

Name	$z$	Stellar corr.	$V$ ( $\text{km s}^{-1}$ )	FWHM ( $\text{km s}^{-1}$ )	$\frac{\lambda 5007}{H\beta}$	$H\beta$ (%)	Stellar corr.	$V$ ( $\text{km s}^{-1}$ )	FWHM ( $\text{km s}^{-1}$ )	$\frac{\lambda 6583}{H\alpha}$	$\frac{\lambda 6300}{H\alpha}$	$H\alpha$ (%)	$\Delta V$ ( $\text{km s}^{-1}$ )	Class.
Mark 938	0.019	A	111	240	1.18	91	T	173	270	0.71	0.07	89	-62	H II
			(-79)	890	(10)	9		-11	648	6.78	< 0.3	11	-68	Sey2
Mark 957	0.0732		-402	710	9.00	8		-201	726	1.35	< 0.3	18	-201	Sey2
			-43	200	0.15	92		3	192	0.35	< 0.02	82	-46	H II
IRAS 01346-0924	0.070		114	178	2.13	38		165	148	0.70	< 0.04	23	-51	H II
			-83	< 80	0.83	39		-33	219	0.46	0.07	37	-50	H II
			-224	1069	(10)	23		-	-	-	-	-	-	Sey2
			-	-	-	-		219	2640	-	-	40	-	Sey1
Mark 1066	0.0122		-116	348	12.38	11		-51	270	0.77	0.07	35	-65	Sey2
			30	220	1.54	66		54	205	0.89	0.08	39	-24	H II
			-262	875	5.76	23		-165	(875)	1.49	0.15	26	-97	Sey2
IRAS 03355+0104	0.0398		-1	364	13.69	100		12	354	0.49	0.12	66	-13	Sey2
			-	-	-	-		264	1930	-	-	34	-	Sey1
IRAS 04210+0400	0.0462		14	178	13.30	41		63	219	0.40	0.17	47	-49	Sey2
			0	541	13.03	59		41	615	0.34	0.06	53	-41	Sey2
IRAS 04507+0358	0.0296		-28	240	11.00	82		14	282	0.47	0.09	64	-42	Sey2
			-146	603	14.57	18		-	-	-	-	-	-	Sey2
			-	-	-	-		-88	1254 $l_z$	-	-	36	-	Sey1
VII Zw 73	0.0405		0	307	(15)	28		17	272	0.80	0.10	37	-17	Sey2
			-186	794	(15)	12		-171	685	0.52	0.22	16	15	Sey2
			3	151	1.28	60		14	111	0.48	0.02	47	-11	H II
Mark 622	0.0233	T, A	6	178	(0.1)	59	T	12	205	0.79	0.06	49	-6	H II
			-58	1172	(10)	41		-22	748	1.44	< 0.5	51	-36	Sey2
3C 198.0	0.081		-	-	-	-	125	294	0.28	0.05	100	-	?	
KUG 0825+248	0.083		108	< 80	0.62	100	135	95	0.29	0.02	100	-27	H II	
IRAS 09111-1007 E	0.055		-113	< 80	(0.1)	16		-230	95	0.55	< 0.09	12	117	H II
			(-76)	259	(0.1)	53		-41	257	0.86	< 0.05	40	-35	H II
			-113	430	(10)	31		-96	626	0.95	0.12	48	-17	Sey2
Zw 238.066	0.034	T, A	95	220	0.60	54	A	149	< 80	0.69	< 0.05	14	-54	H II
			-134	154	1.33	37		-71	307	0.79	0.05	78	-63	H II
			-295	935	(10)	9		-529	1130	3.75	< 0.6	8	234	Sey2

**Table 6.** Fitting profile analysis results (continued).

Name	$z$	Stellar corr.	$V$ ( $\text{km s}^{-1}$ )	FWHM ( $\text{km s}^{-1}$ )	$\frac{\lambda 5007}{\text{H}\beta}$	$\text{H}\beta$ (%)	Stellar corr.	$V$ ( $\text{km s}^{-1}$ )	FWHM ( $\text{km s}^{-1}$ )	$\frac{\lambda 6583}{\text{H}\alpha}$	$\frac{\lambda 6300}{\text{H}\alpha}$	$\text{H}\alpha$ (%)	$\Delta V$ ( $\text{km s}^{-1}$ )	Class.
UGC 5101 #1	0.039		–	–	–	–		254	95	0.51	0.05	100	–	H II
UGC 5101 #2			–	–	–	–		222	163	0.51	0.05	85	–	H II
			–	–	–	–		101	526	2.57	< 0.4	15	–	Sey2
UGC 5101 #3			–	–	–	–		146	132	0.51	0.07	28	–	H II
			–	–	–	–		92	481	4.50	0.14	14	–	Sey2
			–	–	–	–		197	1033 <sub><math>l_z</math></sub>	–	–	58	–	Sey1
UGC 5101 #4			–	–	–	–		–108	148	0.70	< 0.13	15	–	H II
			–	–	–	–		87	114	0.38	< 0.09	21	–	
			–	–	–	–		36	492	5.33	< 0.4	10	–	
			–	–	–	–		324	1438 <sub><math>l_z</math></sub>	–	–	54	–	Sey1
UGC 5101 #5			–	–	–	–		–3	401	1.31	< 0.12	34	–	Sey2
			–	–	–	–		–119	148	0.52	0.06	66	–	H II
UGC 5101	0.039	A	92	364	2.17	100		–	–	–	–	–	–	
NGC 2989	0.014	A	–105	128	1.70	100		–108	148	0.53	0.04	100	3	H II
CG 49	0.044	A	–67	259	7.20	100		–40	257	0.80	0.09	100	–27	Sey2
NGC 3185	0.004	A	12	154	4.68	74	A	68	148	0.81	0.04	66	–56	?
			–164	154	2.03	26		–78	114	0.64	< 0.03	34	–86	H II
Arp 107A	0.034		–	–	–	–		141	178	1.41	0.20	54	–	Sey2
			–	–	–	–		108	492	1.23	< 0.1	46	–	Sey2
NGC 3504	0.005	T, A	–47	200	(0.1)	95	A	0	192	0.58	0.02	93	–47	H II
			–10	398	(10)	5		12	582	1.87	0.08	7	–22	Sey2
IRAS 11058–1131	0.0547		–9	259	7.57	100		65	205	0.34	0.05	76	–74	Sey2
			–	–	–	–		399	2071	–	–	24	–	Sey1
NGC 3642	0.005	T	44	98	0.14	88		71	95	0.48	0.07	39	–27	H II
			50	(330)	(10)	12		36	330	1.00	< 0.3	9	14	Sey2
			–	–	–	–		–10	2168	–	–	52	–	Sey1
Mark 1291	0.0122		–70	154	3.84	100		–4	178	0.73	0.04	50	–66	?
			–	–	–	–		–54	1941	–	–	50	–	Sey1
IRAS 11285+8240 A	0.028		–	–	–	–		141	205	0.45	0.11	100	–	Sey2
Mark 739 W	0.0297	A	9	< 80	0.27	90	A	14	95	0.49	0.02	44	–5	H II
			–4	259	8.77	10		–38	307	0.67	0.10	18	34	Sey2
			–	–	–	–		–57	2103	–	–	38	–	Sey1
SBS 1136+594	0.0613		–38	154	11.66	10		6	192	0.10	0.18	9	–44	Sey2
			–105	4470	–	90		–21	3871	–	–	83	–84	Sey1
			–	–	–	–		–23	1010	–	–	8	–	Sey1
NGC 3994	0.010	T	98	200	0.82	89	T	77	192	0.53	0.05	70	21	H II
			–64	905	6.00	11		33	537	1.41	0.53	30	–99	Liner
NGC 4102	0.0025	T	–25	154	0.43	93	A	57	192	0.87	–	79	–82	H II
			–126	557	(10)	7		–19	(557)	1.57	–	6	–107	Sey2
			–	–	–	–		273	132	0.94	–	15	–	?



**Table 6.** Fitting profile analysis results (continued).

Name	$z$	Stellar corr.	$V$ (km s <sup>-1</sup> )	FWHM (km s <sup>-1</sup> )	$\lambda 5007$ H $\beta$	H $\beta$ (%)	Stellar corr.	$V$ (km s <sup>-1</sup> )	FWHM (km s <sup>-1</sup> )	$\lambda 6583$ H $\alpha$	$\lambda 6300$ H $\alpha$	H $\alpha$ (%)	$\Delta V$ (km s <sup>-1</sup> )	Class.
IRAS 12474+4345 S	0.062		182	200	2.24	53		128	178	0.45	0.05	47	54	H II
			125	478	4.43	47		77	458	0.40	0.03	53	48	?
UGC 8621	0.020	T	3	< 80	0.28	83		54	< 80	0.42	< 0.01	55	-51	H II
			-141	664	(10)	17	-21	(664)	1.78	< 0.3	9	-120	Sey2	
Mark 266 NE	0.0283		-	-	-	-		-238	2987	-	-	36	-	Sey1
			-88	313	0.96	63		-	-	-	-	-	-	H II
Mark 266 SW	0.0278		-278	1009	2.17	37		-	-	-	-	-	-	Liner?
			-125	200	3.65	46		-61	270	0.58	0.06	58	-64	?
Mark 1361	0.0224		114	295	0.36	33		186	270	0.58	0.04	31	-72	H II
			-110	603	13.30	21		-259	(603)	0.49	0.12	11	149	Sey2
Mark 461	0.016	T	108	178	(0.1)	51		260	95	0.54	0.05	15	-152	H II
				17	277	9.17	31		117	192	0.66	0.04	49	-100
4C 26.42	0.063	T	-142	785	(10)	18		54	548	1.04	0.09	26	-196	Sey2
				-	-	-	-		68	2427	-	-	10	-
I Zw 81	0.052	A	114	313	0.99	66		74	219	0.60	-	37	40	H II
				-31	920	> 2.6	34		41	692	0.64	-	63	-72
Mark 477	0.038	A	-267	(342)	0.42	52		-173	(342)	0.83	0.20	62	-94	Liner
				47	(220)	0.62	48		159	(220)	0.86	0.27	38	-112
Mark 848 S	0.040	A	17	(132)	2.05	53		98	132	0.78	< 0.04	43	-81	H II?
				-226	(132)	1.41	47		-122	132	0.56	< 0.03	57	-104
IRAS 15184+0834	0.031	A	-108	200	8.00	30		-53	163	0.38	0.15	31	-55	Sey2
				-83	478	11.05	47		-26	481	0.31	0.22	47	-57
NGC 5953	0.007	T, A	-238	1600	13.01	23		-379	(1600)	0.74	0.23	22	141	Sey2
				81	154	0.83	93		128	132	0.43	0.03	81	-47
Kaz 49	0.030	A	-92	680	4.20	7		122	469	0.71	0.14	19	-214	Sey2
				-286	(178)	1.35	18		-203	178	0.54	0.01	21	-83
IRAS 16129-0753	0.033	A	-6	220	4.70	82		9	257	0.69	0.05	79	-15	?
				-92	200	0.55	88		-36	205	0.60	0.03	54	-56
IRAS 16382-0613	0.028	A	-185	398	(10)	12		-128	412	1.96	0.18	22	-57	Sey2
				-	-	-	-		311	1768	-	-	24	-
IRAS 16129-0753	0.033	A	57	259	2.21	88		144	232	0.55	0.05	88	-87	H II
				-252	1069	(10)	12		-218	879	2.05	< 0.5	12	-34
IRAS 16382-0613	0.028	A	-166	154	0.33	84		-85	205	0.59	< 0.05	100	-81	H II
				-218	649	11.25	16		-	-	-	-	-	-
IRAS 16382-0613	0.028	A	-76	348	3.94	40		-72	257	0.91	< 0.03	24	-6	?
				-310	1157	4.06	60		-188	1064	1.41	< 0.12	24	-122
			-	-	-	-		144	4980	-	-	52	-	Sey1

**Table 6.** Fitting profile analysis results (end).

Name	$z$	Stellar corr.	$V$ (km s <sup>-1</sup> )	FWHM (km s <sup>-1</sup> )	$\lambda 5007$ H $\beta$	H $\beta$ (%)	Stellar corr.	$V$ (km s <sup>-1</sup> )	FWHM (km s <sup>-1</sup> )	$\lambda 6583$ H $\alpha$	$\lambda 6300$ H $\alpha$	H $\alpha$ (%)	$\Delta V$ (km s <sup>-1</sup> )	Class.
Mark 700	0.034	A	-74	618	1.86	100		-28	435	2.19	0.19	23	-46	Liner
			-	-	-	-		369	1595	-	-	61	-	Sey1
			-	-	-	-		-1137	1097	-	-	16	-	Sey1
MCG 03.45.003	0.024		87	98	14.01	47		77	132	0.51	0.17	54	10	Sey2
			27	364	8.71	53		39	435	0.61	< 0.07	46	-12	Sey2
PGC 61548	0.018	T	20	277	0.41	92		68	282	0.50	0.04	93	-48	H II
			-5	541	(10)	8		14	604	3.94	0.49	7	-19	Sey2
Kaz 214	0.046	A	0	< 80	5.32	10		-	-	-	-	-	-	?
			98	330	3.60	73		-	-	-	-	-	-	?
			195	740	(10)	17		-	-	-	-	-	-	-
Kaz 214 #1			-	-	-		-25	95	0.32	< 0.06	100	-	H II	
Kaz 214 #2			-	-	-		-28	148	0.38	< 0.05	100	-	H II	
Kaz 214 #3			-	-	-	-		12	245	0.52	< 0.05	68	-	H II
			-	-	-	-		(120)	(525)	(0.60)	0.17	32	-	Sey2?
Kaz 214 #4			-	-	-	-		77	205	0.33	< 0.03	60	-	H II
			-	-	-	-		(120)	(525)	(0.60)	0.16	40	-	Sey2?
Kaz 214 #5			-	-	-	-		114	132	0.28	< 0.02	45	-	H II
			-	-	-	-		(120)	(525)	(0.60)	0.09	55	-	Sey2?
Kaz 214 #6			-	-	-	-		135	114	0.31	0.05	44	-	H II
			-	-	-	-		(120)	(525)	(0.60)	0.16	56	-	Sey2?
Kaz 214 #7			-	-	-	-		141	232	0.35	< 0.06	100	-	H II
NGC 6764	0.008		47	330	0.62	72		-7	319	0.65	0.04	66	54	H II
			-158	430	0.44	28		-101	537	0.96	0.14	34	-57	Liner
IRAS 22114-1109	0.054		44	154	1.33	46		-16	219	0.70	< 0.07	57	60	H II
			195	510	(10)	54		203	319	0.60	0.12	43	-8	Sey2
Mark 308	0.023		155	178	(0.1)	56		87	132	0.30	0.06	44	68	H II
			243	240	(10)	24		63	412	0.49	0.03	30	180	Sey2?
			182	995	(10)	20		-34	1097	0.50	0.19	19	216	Sey2
Mark 522	0.032	A	-	-	-	-		(23)	(1725)	-	-	7	-	Sey1
			95	< 80	0.63	86		114	114	0.53	< 0.04	75	-19	H II
			-15	220	7.87	14		30	270	1.50	< 0.2	25	-45	Sey2
Mark 313	0.006	A	128	154	2.29	100		117	114	0.44	0.10	74	11	H II
			-	-	-	-		84	424	0.71	0.28	26	-	Sey2?
Zw 453.062	0.025	A	20	200	0.31	94		-42	163	0.46	0.05	91	62	H II
			-274	541	(10)	6		-160	514	3.33	0.4	9	114	Sey2
IC 5298	0.027	T	95	313	0.53	76		44	307	0.83	0.12	86	51	H II
			-68	557	(10)	24		33	537	2.28	< 0.4	14	-101	Sey2

The line fitting analysis of the spectra was done in terms of Gaussian components as described in Véron et al. (1980, 1981b,c). The three emission lines,  $H\alpha$  and  $[\text{N II}]\lambda\lambda 6548, 6583$  (or  $H\beta$  and  $[\text{O III}]\lambda\lambda 4959, 5007$ ) were fitted by one or several sets of three Gaussian components; whenever necessary, two components were added to fit the  $[\text{O I}]\lambda\lambda 6300, 6363$  lines. The width and redshift of each component in a set were supposed to be the same. The intensity ratios of the  $[\text{N II}]\lambda\lambda 6548, 6583$ ,  $[\text{O III}]\lambda\lambda 4959, 5007$  and  $[\text{O I}]\lambda\lambda 6300, 6363$  lines were taken to be equal to 3.00, 2.96 and 3.11, respectively (Osterbrock 1974). Whenever a fit resulted in a small negative intensity for a  $H\beta$  component, we set the corresponding  $\lambda 5007/H\beta$  ratio to 10, the mean value for Seyfert 2s.

All line widths given in this paper have been corrected for the instrumental broadening. The spectra and best fits are plotted in Fig. 1, the parameters describing the individual components required by the analysis being given in Table 6.

### 2.3. Notes on individual objects

**Mark 938.** This galaxy is apparently undergoing a merger as evidenced by the presence of tidal tails (Mulchaey et al. 1996; Mazzarella & Boroson 1993). The nature of its emission-line spectrum has been rather controversial. Afanasjev et al. (1980) classified it as a Seyfert 2, Osterbrock & Dahari (1983) claimed that it is not a Seyfert; Dahari (1985), Véron-Cetty & Véron (1986a) and Veilleux et al. (1995) called it again a Seyfert 2, while Mulchaey et al. (1996), observing a weak emission of  $[\text{O III}]\lambda 5007$  and a strong  $H\alpha$  over the entire galaxy, suggested that there is no Seyfert activity in this object, in agreement with Mazzarella & Boroson (1993) who called it a H II region. The line ratios published by Veilleux et al. (1995) and Vaceli et al. (1997) indicate a “transition” spectrum, the  $[\text{O III}]$  lines being weak for a Seyfert 2 galaxy ( $\lambda 5007/H\beta = 4$ ). The high resolution spectroscopic observations of Busko & Steiner (1990), showing complex emission line profiles with great differences in width and shape between  $H\alpha$  and  $[\text{N II}]\lambda 6583$  (the measured line widths are  $264 \pm 7$  and  $384 \pm 12 \text{ km s}^{-1}$  for  $H\alpha$  and  $[\text{N II}]\lambda 6583$ , respectively), suggest a “composite” spectrum. To fit our spectra, two components are needed: one is a H II region with narrow lines ( $\sim 255 \text{ km s}^{-1}$  FWHM); the other is a Seyfert 2 with much broader lines ( $\sim 760 \text{ km s}^{-1}$  FWHM). For this component, we find a very high and unlikely  $\lambda 6583/H\alpha$  ratio ( $\sim 6.8$ ); however, there is a very strong and broad  $H\beta$  absorption line. It is probable that the broad  $H\alpha$  emission component intensity is greatly reduced by the presence of a  $H\alpha$  absorption line which has not been accounted for.

**Mark 957.** This galaxy has been identified with the radio source 5C 3.100 (Antonucci 1985) and a ROSAT X-ray source (Boller et al. 1998). Dahari & de Robertis (1988) called it a Seyfert 2. However, Koski (1978) and Halpern & Oke (1987) have observed strong Fe II emission lines in this object; furthermore, the continuum is very flat, extending far into the blue (Koski 1978), accounting for the classification of this object as a Narrow Line Seyfert 1 galaxy. This classification is supported by Boller et al. (1996) who have found a steep

soft X-ray component (photon index  $\Gamma = 2.9 \pm 0.2$ ) with a variable flux (by a factor 1.9 over 18900 sec). The  $H\beta$  line is very narrow (FWHM  $< 685 \text{ km s}^{-1}$ ) (Goodrich 1989); narrow  $H\alpha$  and  $[\text{N II}]$  lines are observed as far as  $10''$  from the nucleus (with  $\lambda 6583/H\alpha \sim 0.4$ ) (Halpern & Oke 1987), suggesting the presence of an extended H II region. In the nucleus, the high ionization lines ( $[\text{O III}]$  and  $[\text{Ne III}]\lambda 3869$ ) are found to be blueshifted by  $\sim 280 \text{ km s}^{-1}$  with respect to the low ionization lines. Although having a relatively low signal-to-noise ratio, our spectra are quite interesting. In the blue, there is a very narrow  $H\beta$  emission line (FWHM  $\sim 200 \text{ km s}^{-1}$ ) associated with very weak ( $\lambda 5007/H\beta \sim 0.15$ ) and relatively broad (FWHM  $\sim 710 \text{ km s}^{-1}$ )  $[\text{O III}]$  lines; the associated broad  $H\beta$  component is weak ( $\lambda 5007/H\beta \sim 9$ ) and accounts for only 8% of the total  $H\beta$  flux. The  $[\text{O III}]$  lines are blueshifted by  $\sim 360 \text{ km s}^{-1}$  with respect to  $H\beta$ . The red spectrum is also reasonably fitted with two sets of components; one is narrow with weak  $[\text{N II}]$  lines, while the second is broader with relatively strong  $[\text{N II}]$  lines. This is in satisfactory agreement with Halpern & Oke’s results, and suggests that the nuclear spectrum is dominated by a strong H II region superimposed onto a relatively weak Seyfert 2 nucleus.

**IRAS 01346 - 0924** was identified by de Grijp et al. (1987) with a galaxy they called MCG  $-02.05.022$ , which seems to be erroneous. It was classified a Seyfert 2 by de Grijp et al. (1992) on the basis of its emission-line ratios. We discussed this object in Paper I, giving it the wrong name (MCG  $-02.05.022$ ); we suggested, on the basis of a blue spectrum, that it was “composite”. The best blue spectrum fit is obtained with three sets of three Gaussians, two being typical of a H II region and the third of a weak Seyfert 2 nebulousity. A weak broad (FWHM  $\sim 2640 \text{ km s}^{-1}$ )  $H\alpha$  component may also be present. The Seyfert 2 cloud is so weak that it is not detected on our red spectrum.

**Mark 1066** is an early-type spiral galaxy (Afanasjev et al. 1981; Mazzarella & Boroson 1993). It was classified as a Seyfert 2 by Afanasjev et al. (1980) and as a Seyfert 1.9 by Afanasjev et al. (1981) on the basis of weak broad components in the Balmer lines; the existence of these broad components has not been confirmed by Goodrich & Osterbrock (1983) who concluded, on the basis of the line ratios ( $\lambda 5007/H\beta = 4.35$ ,  $\lambda 6583/H\alpha = 0.88$ ,  $\lambda 6300/H\alpha = 0.08$ ), that this object is a Seyfert 2. However, Osterbrock & Dahari (1983), on the basis of the same data, called it a “marginal” Seyfert 2, the  $\lambda 5007/H\beta$  ratio being relatively weak. The spectra published by Wilson & Nath (1990) and Veilleux (1991a) show that the emission lines have a broad blue wing extending up to velocities of  $1000 \text{ km s}^{-1}$  with respect to the line peaks, the  $[\text{O III}]$  lines being significantly broader ( $403 \text{ km s}^{-1}$  FWHM) than the Balmer lines ( $280 \text{ km s}^{-1}$ ) (Veilleux 1991b,c). De Robertis & Osterbrock (1986) noted a good correlation between the width of the line at half-peak intensity and the critical density, suggesting that the narrow line region (NLR) is density stratified; however, the density stratification mostly affects the high velocity gas producing the wings of the line profiles (Veilleux 1991c). Haniff et al. (1988) have published an  $[\text{O III}]$  image suggestive of a double structure with a separation of  $0''.8$ ,

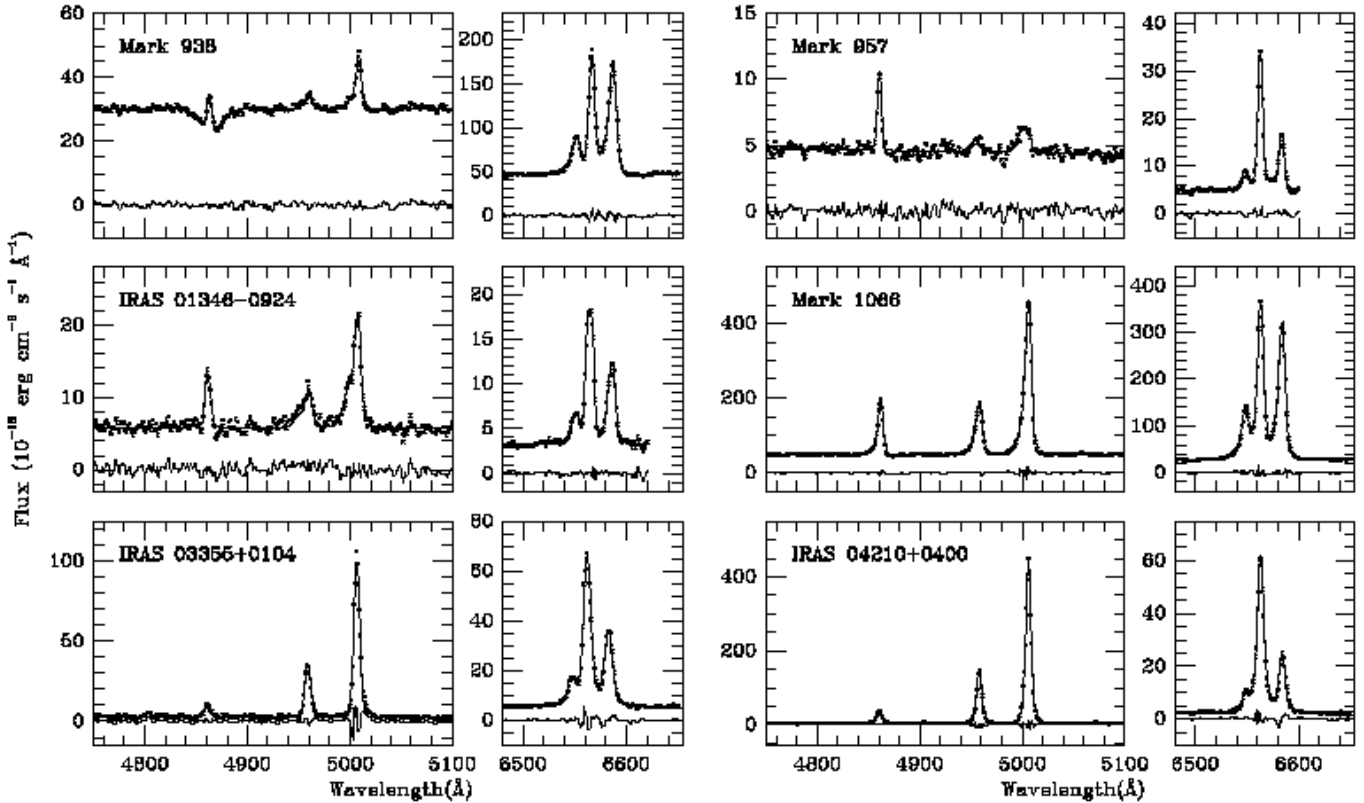


**Fig. 1.** Blue and red spectra for the 53 galaxies studied in this paper. For 52 of the observed AGNs we present  $66 \text{ \AA mm}^{-1}$  spectra; in the case of VII Zw 73, we give  $33 \text{ \AA mm}^{-1}$  spectra. For 4 of the observed objects, only one spectral region is available. All the spectra were de-redshifted to rest wavelengths. The spectral ranges displayed are  $\lambda\lambda 4750\text{--}5120 \text{ \AA}$  and  $\lambda\lambda 6480\text{--}6650 \text{ \AA}$ . In each frame the data points (small crosses), the best fit (solid line) and the residuals (lower solid line) are shown. For the red spectrum of SBS 1136+594, the individual components of the fit are also given as an example (dotted lines).

and the continuum nucleus in between. There are two emission peaks in the core of the low-ionization lines; these peaks are separated by about  $0''.5$ , the velocity difference between them being  $\Delta V = 125 \pm 20 \text{ km s}^{-1}$  (Veilleux 1991c). High-resolution ( $0''.1$ ) HST images (Bower et al. 1995) reveal that the  $H\alpha$  and  $[\text{N II}]$  emission comes from a  $3''$ -long region centered on the nucleus, while the  $[\text{O III}]$ -emitting gas is concentrated in a bright “jet-like” structure extending  $1''.4$  NW of the nucleus. Long-slit spectroscopy suggests the existence of two kinematically distinct regions: the first, of low-excitation, lies in the plane of the galaxy and is normally rotating, while the second, of high-excitation, would be inclined with respect to the disk. Bower et al. (1995) suggested that the high-ionization cloud is a Seyfert 2 (with  $\lambda 5007/H\beta \sim 10\text{--}15$ ) and the low-ionization cloud is a Liner ( $\lambda 5007/H\beta \sim 2\text{--}3$ ); it seems, however, that the  $[\text{O I}]$  lines are weak and that this region could be a  $\text{H II}$  region instead. Three sets of lines are needed to fit our spectra; one set originates, most probably, from a  $\text{H II}$  region, the two others having line ratios typical of Seyfert 2 clouds. The velocity difference between the two Seyfert components is  $\Delta V = 146 \text{ km s}^{-1}$  in the blue and  $105 \text{ km s}^{-1}$  in the red. The complexity of the line emission regions in this object, revealed by the HST observations, makes the measured line ratios for each individual component rather inaccurate. It seems likely

that the density-stratified cloud emitting relatively broad lines is compact and coincides with the nucleus. This is, therefore, a “composite-spectrum object”.

**IRAS 03355+0104** has been identified by de Grijp et al. (1987) with a galaxy shown to be a Seyfert 2 by de Grijp et al. (1992) who have measured  $\lambda 6583/H\alpha = 0.58$ , a normal value for such an object; however, Vogel et al. (1993) have found much weaker  $[\text{N II}]$  lines, with  $\lambda 6583/H\alpha = 0.18$ . Our red spectrum gives  $\lambda 6583/H\alpha = 0.49$ , in agreement with de Grijp et al. (1992), and  $\lambda 6300/H\alpha = 0.12$ , so this object is a Seyfert 2 galaxy. In addition, a weak broad  $H\alpha$  component seems to be present, in which case it would be a Seyfert 1.9 galaxy.

**IRAS 04210+0400** has been identified with a compact blue galaxy with a faint blue, spiral companion (Moorwood et al. 1986). It is associated with a double lobed radio source, 20–30 kpc in size (Beichman et al. 1985; Hill et al. 1988). The galaxy has an apparent spiral structure (Beichman et al.); however, these features are dominated by emission lines, and the galaxy is probably an elliptical (Hill et al. 1988; Steffen et al. 1996).

We have searched the *Hubble Space Telescope* archives and found images obtained with the Wide Field Planetary Camera 2, on January 31, 1995 through medium and broad band filters

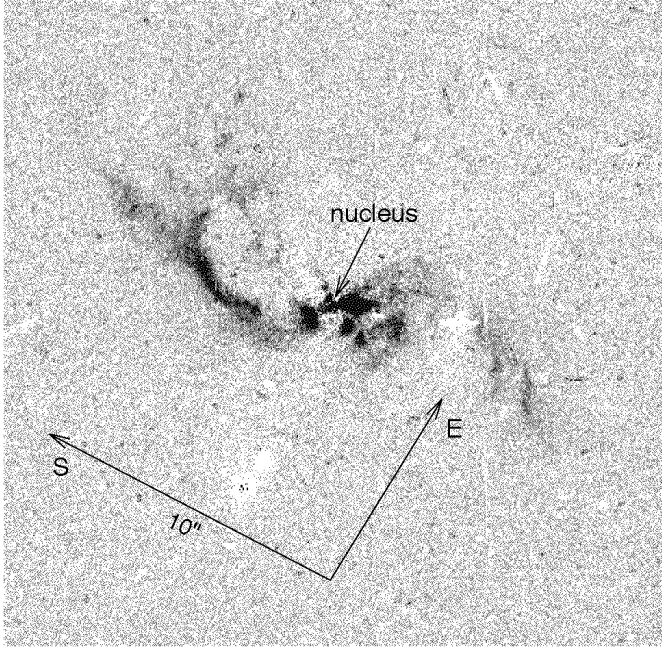


**Fig. 2.**  $H\alpha$ + $[N II]$  *HST* image of IRAS 04210+0400, after removal of the continuum. The nucleus is indicated by an arrow.  $10''$ , given as a reference on the image, correspond to 13.5 kpc at the distance of the galaxy (assuming  $H_0 = 50 \text{ km s}^{-1} \text{ Mpc}^{-1}$ ).

isolating several emission lines and a line-free continuum. We retrieved and analysed these unpublished images, the *HST* observing log being given in Table 7. The galaxy was imaged on the Planetary Camera, a  $800 \times 800$  pixels CCD with a read-out noise of  $\sim 5 \text{ e}^- \text{ pixel}^{-1}$ . The pixels size is  $15 \times 15 \mu\text{m}$ , which corresponds to  $0''.0455$  on the sky; the field is  $36''.4 \times 36''.4$  (Trauger et al. 1994; Holzman et al. 1995).

Both the  $H\alpha$ + $[N II]$  and the  $[O III]$  images (after subtraction of the continuum) show a very complex structure with a bright unresolved nucleus, a relatively bright elongated central region extending over  $\sim 2''.4$ , made of several distinct clouds, and a thin spiral feature with a total extent of about  $15''$  (Fig. 2).

The Balmer decrement observed over a  $2'' \times 2''$  area centered on the nucleus is relatively large ( $H\alpha/H\beta = 5.5$ ) (Hill et al. 1988), implying a large extinction ( $A_V \sim 1.4 \text{ mag}$ ). We cannot exclude the possibility that the extinction varies over the emission nebulosity; therefore, the ratio  $(H\alpha + [N II])/\lambda 5007$ , which is approximately equal to  $H\alpha/\lambda 5007$  as  $[N II]\lambda 6583 \sim 1/3 H\alpha$ , cannot be taken as an estimate for the excitation parameter  $\lambda 5007/H\beta$ . Our entrance aperture ( $2''.1 \times 5''.0$ ), with the slit oriented in the E-W direction, basically includes the central point source and the bright central nebulosity.

Published nuclear line ratios (Hill et al.) led to the classification of this object as a Seyfert 2 (Beichman et al. 1985; Holloway et al. 1996) although  $\lambda 6583/H\alpha = 0.35$ , a low value for this class. The core region shows asymmetric spatial structure with several separate components in velocity and space; there are systematic shifts between peak positions for the different lines (Holloway et al. 1996). Our spectra basically confirm the

line ratios obtained in the nuclear region. This is a Seyfert 2 galaxy with abnormally weak  $[N II]$  emission lines.

**Table 7.** *HST* observing log of IRAS 04210+0400.

ID label	Band	$\lambda_c$ ( $\text{\AA}$ )	$\Delta\lambda$ ( $\text{\AA}$ )	Filter	Time (s)
u2mg0401t	[O III]	5479	486	F547 M	300
u2mg0402t	[O III]	5479	486	F547 M	300
u2mg0403t	continuum	7940	1531	F814 W	600
u2mg0404t	$H\alpha$ + $[N II]$	6814	877	F675 W	600

**IRAS 04507+0358** has been identified with an elliptical galaxy (de Grijp et al. 1987) shown to be a Seyfert 2 by de Grijp et al. (1992) who, however, have measured  $\lambda 6583/H\alpha = 0.28$ , a very low value for an object of such a class. Our red spectrum gives  $\lambda 6583/H\alpha = 0.47$  with, perhaps, a weak broad Lorentzian  $H\alpha$  component. Therefore, this is not a “composite-spectrum object”, but rather a Seyfert 2 galaxy or perhaps a Seyfert 1.9, if the broad component is confirmed.

**VII Zw 73** has been classified as a Seyfert 2 galaxy by de Grijp et al. (1992) on the basis of its emission line ratios ( $\lambda 5007/H\beta = 3.96$ ,  $\lambda 6583/H\alpha = 0.56$ ); however, as in the case of Mark 1066, the  $[O III]\lambda 5007$  line is rather weak for a Seyfert 2. Our blue spectrum shows  $H\beta$  to be clearly narrower than the  $[O III]$  lines, an indication of the probable “composite” nature of this galaxy. To obtain a good fit to our blue and red spectra, three components are needed. However, two of these components turned out to have similar velocities and widths, making the determination of the line ratios rather uncertain. We therefore re-observed this galaxy with a higher resolution ( $33 \text{ \AA mm}^{-1}$ ) in the red on October 29, 1997 and in the blue on October 30. Again three components were needed to fit the spectra, but this time they were clearly identified as corresponding to two Seyfert 2 nebulosities and a  $H II$  region.

**Mark 622.** The line ratios published by Shuder & Osterbrock (1981) show that it is a Seyfert 2 galaxy, although the  $[O I]\lambda 6300$  relative flux is too low for such a class ( $\lambda 6300/H\alpha = 0.06$ ). Furthermore, these authors found that the  $[O III]$  lines are much broader ( $\text{FWHM} \sim 1050 \text{ km s}^{-1}$ ) than the  $H\alpha$ ,  $[N II]$  and  $[O II]$  lines ( $\text{FWHM} \sim 350 \text{ km s}^{-1}$ ) suggesting the presence of two emission-line regions of different ionization. Wilson & Nath (1990) have shown that, in the nucleus, the  $[N II]$  lines are broader than  $H\alpha$  ( $\text{FWHM} = 340 \pm 20$  and  $240 \pm 20 \text{ km s}^{-1}$  respectively); moreover, the  $[O III]$  image of this object is only slightly resolved, while  $\sim 60\%$  of the  $H\alpha$  emission comes from an extended component (Mulchaey et al. 1996). Our spectra confirm these results; in fact, two components are needed in order to obtain a good fit: one is representative of a  $H II$  region, the other is typical of a Seyfert 2 cloud.

**3C 198.0.** The line ratios in this elliptical radio galaxy are those of a  $H II$  region, as discussed in Paper I. Our measurements are in agreement with the published values:  $\lambda 6300/H\alpha = 0.05$  and  $\lambda 6583/H\alpha = 0.28$ . This is therefore a really puzzling object.

**KUG 0825 +248.** The published emission-line relative intensities (Augarde et al. 1994) are typical of a H II region except for the [O I] lines, which are too strong ( $\lambda 6300/\text{H}\alpha = 0.13$ ). On our red spectrum, we measured  $\lambda 6300/\text{H}\alpha = 0.02$ . Our values for  $\lambda 5007/\text{H}\beta$  and  $\lambda 6583/\text{H}\alpha$  are in agreement with the published values. This object is, therefore, a typical H II region.

**IRAS 09111-1007** has been identified with the western component of a galaxy pair (Murphy et al. 1996). The eastern component, separated by  $40''$ , is called IRAS 09111-1007E, although it is probably unrelated to the IR source; it has a “transition” spectrum with  $\lambda 5007/\text{H}\beta = 3.94$ ,  $\lambda 6583/\text{H}\alpha = 0.74$  and  $\lambda 6300/\text{H}\alpha = 0.07$  (Duc et al. 1997). Our observations suggest that the spectrum of this object is indeed “composite”, the [O III] lines being broader than H $\beta$ . The blue spectrum CCD image clearly shows the H $\beta$  line to be double and spatially resolved. In fact, to obtain a good fit to the H $\alpha$ + [N II] and H $\beta$ + [O III] lines, three components are needed: one with line ratios typical of a Seyfert 2 cloud, and the two others typical of H II regions.

**Zw 238.066.** On the basis of the published line intensity ratios, Veilleux et al. (1995) have called this object a Liner; however, the [O I] lines are weak ( $\lambda 6300/\text{H}\alpha = 0.07$ ). Our observations suggest that it has a “composite” nature. The red spectrum image clearly shows the H $\alpha$  and [N II] lines to be extended, with a low relative intensity of the [N II] lines. The blue spectrum shows that the [O III] lines have a broad blue wing not seen in H $\beta$ . We have therefore fitted both the red and blue spectra with three sets of lines. The blue spectrum has a rather poor signal-to-noise ratio which probably explains why the parameters of the blue and red fits (especially the line widths) are not in good agreement; however, the differences of profile of the different lines leave no doubt about the “composite” nature of this spectrum. Indeed, the fits show that the emission-line spectrum is dominated by two H II clouds separated by  $\sim 220 \text{ km s}^{-1}$ ; but there is, in addition, a weak Seyfert 2 nebulousity with relatively broad lines ( $\sim 1030 \text{ km s}^{-1}$  FWHM).

**UGC 5101.** This is an ultra-luminous infrared galaxy ( $L_{\text{IR}} \geq 10^{12} L_{\odot}$ ); it is a peculiar galaxy with a large ring and a 15 kpc tidal tail extending to the west, which suggests a merger, although no companions are known to this galaxy. It has a single bright nucleus (Sanders et al. 1988). Optical spectra have been published by Sanders et al. who classified it as a Seyfert 1.5 galaxy on the basis of a relatively broad H $\alpha$  line, by Veilleux et al. (1995) and Wu et al. (1998a,b) who called it a Liner, and by Liu & Kennicutt (1995). However, the published line ratios ( $\lambda 5007/\text{H}\beta = 2.9\text{--}4.7$ ,  $\lambda 6583/\text{H}\alpha = 1.17\text{--}1.35$ ,  $\lambda 6300/\text{H}\alpha = 0.06\text{--}0.09$ ) rather indicate a “transition” spectrum. Our red slit spectrum (PA =  $270^\circ$ ) shows spatially extended narrow emission lines with a steep velocity gradient across the nucleus in addition to broader, spatially unresolved lines in the nucleus itself. We have extracted five columns centered on the nucleus and analysed separately the five spectra. In each case, we have found a narrow component (FWHM  $\sim 100\text{--}150 \text{ km s}^{-1}$ ) with  $\lambda 6583/\text{H}\alpha \sim 0.50$  and  $\lambda 6300/\text{H}\alpha \sim 0.05$ , the velocity decreasing from  $\sim 250$  (West) to  $-120 \text{ km s}^{-1}$  (East). On three

spectra, we detected relatively broad (FWHM  $\sim 500 \text{ km s}^{-1}$ ) lines, with  $\lambda 6583/\text{H}\alpha > 1$  and  $\lambda 6300/\text{H}\alpha < 0.40$ . In addition, on the two central spectra, there is a weak, broad (FWHM  $\sim 1200 \text{ km s}^{-1}$ ) H $\alpha$  component. It was not possible to perform such a detailed analysis on the blue spectrum, which has a much lower signal-to-noise ratio due to a large Balmer decrement (H $\alpha/\text{H}\beta = 8.3$ ; Sanders et al. 1988). Nevertheless, we can draw some conclusions: the medium width H $\alpha$  component flux, coadded on the three central columns, represents 24% of the total H $\alpha$  flux on the same three columns (excluding the broad H $\alpha$  component); assuming that the Balmer decrement is the same for the narrow and medium width components, and that the narrow component is a H II region (this component having  $\lambda 6583/\text{H}\alpha \sim 0.50$ , must have  $\lambda 5007/\text{H}\beta < 2$ ), we conclude that the intermediate width lines set must have  $\lambda 5007/\text{H}\beta > 3.5$  and is, therefore, a Seyfert 2 cloud. So, UGC 5101 has a “composite” spectrum with a rather strong starburst component and a Seyfert 1.8 or 1.9 nucleus (we are not able to decide between 1.8 or 1.9 as, because of the rather poor signal-to-noise ratio around H $\beta$ , it is not possible to put a significant upper limit to the broad H $\beta$  component flux).

**NGC 2989** is a Sc galaxy (Sandage & Bedke 1994). Published data (Table 2) indicate a “transition” spectrum; Phillips et al. (1983) called it a intermediate object, but Véron-Cetty & Véron (1984), on the basis of the same line ratios, classified it as a H II region. Our measured flux ratios ( $\lambda 5007/\text{H}\beta = 1.70$ ,  $\lambda 6300/\text{H}\alpha = 0.04$  and  $\lambda 6583/\text{H}\alpha = 0.53$ ) are in good agreement with Phillips et al. and show that this is indeed a pure H II region with, perhaps a marginally large  $\lambda 6583/\text{H}\alpha$  ratio.

**CG 49.** This galaxy has been shown to have a Seyfert 2 spectrum by Salzer et al (1995); however, they have measured a low relative intensity for the [N II] lines ( $\lambda 6583/\text{H}\alpha = 0.30$ ) as the redshifted wavelength of [N II] $\lambda 6583$  is  $6873 \text{ \AA}$  and falls on the atmospheric B band. After correction for this absorption, our spectrum gives  $\lambda 6583/\text{H}\alpha = 0.80$ , a normal value for a Seyfert 2 galaxy.

**NGC 3185** is a SBa galaxy (Sandage & Bedke 1994). Its emission-line spectrum is power-law photoionized according to Stauffer (1982). Ho et al. (1997a) called it a Seyfert 2, although the published line ratios indicate a “transition” spectrum. We have fitted the lines with two sets of Gaussian profiles: one system is a H II region; the other corresponds to a Seyfert nebulousity, although the [O I] lines are quite weak ( $\lambda 6300/\text{H}\alpha = 0.04$ ).

**Arp 107 A** is the SW component of an interacting galaxy pair (Arp 1966). It exhibits Seyfert 2 activity and its spectrum shows very strong [N II] lines ( $\lambda 6583/\text{H}\alpha = 3.0$ ) according to Keel et al. (1985). Our spectrum shows a more normal value. In fact, the lines have a complex profile which can best be fitted by two sets of Gaussians having different widths, but similar  $\lambda 6583/\text{H}\alpha$  ratios, namely 1.41 and 1.23.

**NGC 3504.** This Sb galaxy (Sandage & Bedke 1994) has a “composite” nucleus showing both non-thermal activity and recent star formation, the optical spectrum being dominated by the regions of stellar activity (Keel 1984). Ho et al. (1993a), who published line ratios for this object, suggested that it could

be a “transition” between a H II region and a Liner, but Ho et al. (1997a) called it a H II region. Fitting our red spectrum with a single set of Gaussians does not give a satisfactory fit and indicates the presence of weak broad wings in the [N II] lines; two sets of Gaussians are needed, revealing the presence of a weak Seyfert-like nebulosity with  $\lambda 6583/H\alpha = 1.87$ . The blue spectrum was also fitted by two sets of Gaussians satisfying, respectively,  $\lambda 5007/H\beta = 0.1$  and  $\lambda 5007/H\beta = 10$ . The NGC 3504 spectrum is therefore “composite” and dominated by a starburst; a weak Seyfert feature is also present. No component showing Liner characteristics was detected in this object.

**IRAS 11058-1131.** In Paper I we concluded, on the basis of a red spectrum, that this object, classified as a Seyfert 2 by various authors (de Grijp et al. 1992, Osterbrock & de Robertis 1985), has weak [N II] lines. Re-analyzing the red spectrum, we have found the possible presence of a weak broad (FWHM  $\sim 2\,100\text{ km s}^{-1}$ )  $H\alpha$  component with 24% of the total  $H\alpha$  flux. Our blue spectrum confirms that this is indeed an AGN with  $\lambda 5007/H\beta = 7.6$  and a relatively strong He II  $\lambda 4686$  line ( $\lambda 4686/H\beta = 0.18$ ). Our conclusion is that IRAS 11058–1131 belongs to the relatively rare class of Seyfert 2 galaxies having weak [N II] lines, discussed in Sect. 4.3; other galaxies belonging to this class are UM 85 and 3C 184.1 (Paper I).

**NGC 3642** is an Sb galaxy (Sandage & Bedke 1994). It was classified as a Liner by Heckman (1980). Filippenko & Sargent (1985) noted the presence of very narrow emission lines (FWHM  $\sim 110\text{ km s}^{-1}$ ) superposed on weak, significantly broader components; a weak broad  $H\alpha$  component was also detected. Koratkar et al. (1995) confirmed the presence of the broad  $H\alpha$  component and called this object a Liner, although their published line ratios rather point to a “transition” spectrum. Our spectra confirm the presence of a broad  $H\alpha$  component (FWHM  $\sim 2\,160\text{ km s}^{-1}$ ) and show, in addition, that the narrow line spectrum is made of two clouds, one with line ratios typical of a H II region and the other of a Seyfert 2 cloud, this object being, therefore, a “composite”.

**Mark 1291.** Spectroscopic observations of this barred spiral by Kollatschny et al. (1983) show it to be a “transition object” between Seyfert 2s and H II regions; however, high excitation lines characteristic of Seyfert 2s such as [Fe XIV]  $\lambda 5303$  and [Fe X]  $\lambda 6374$  are detected. The nuclear emission is compact (Gonzalez Delgado et al. 1997). Our optical spectra show a weak broad (FWHM  $\sim 1\,950\text{ km s}^{-1}$ )  $H\alpha$  component suspected by Kollatschny et al. The narrow lines are well fitted with a single Gaussian profile ( $\sim 160\text{ km s}^{-1}$  FWHM). The line ratios are  $\lambda 5007/H\beta = 3.84$ ,  $\lambda 6300/H\alpha = 0.04$  and  $\lambda 6583/H\alpha = 0.73$  (significantly larger than the published value, 0.48); the classification of this object is therefore ambiguous: it is a Seyfert 2 in the  $\lambda 5007/H\beta$  vs.  $\lambda 6583/H\alpha$  diagram and a H II region in the  $\lambda 5007/H\beta$  vs.  $\lambda 6300/H\alpha$  diagram. It would be of interest to obtain high-resolution, high signal-to-noise spectra of this object to confirm its “transition” nature.

**IRAS 11285+8240 A** has been classified as a Seyfert 2 galaxy by Klaas & Elsasser (1991), with  $\lambda 5007/H\beta = 8.25$  and  $\lambda 6583/H\alpha = 0.46$ . Our red spectrum is well fitted by a single set of components with  $\lambda 6583/H\alpha = 0.45$ , in excellent agree-

ment with the published value, and  $\lambda 6300/H\alpha = 0.11$ . This is another example of Seyfert 2 galaxy with marginally weak [N II] lines.

**Mark 739** has a double nucleus (Petrosian et al. 1978). The eastern nucleus has a Seyfert 1 spectrum (Petrosian et al. 1979; Netzer et al. 1987). The western component, Mark 739 W, has a starburst spectrum according to Netzer et al.; however, Rafanelli et al. (1993) have remarked that  $H\beta$  is unresolved with a resolution of  $130\text{ km s}^{-1}$ , while the [O III] lines are significantly broader ( $\sim 300\text{ km s}^{-1}$  FWHM). Our observations show that this spectrum is indeed “composite” with a Seyfert 2 nucleus and a H II region and, in addition, a weak broad  $H\alpha$  component.

**SBS 1136+594** is a Seyfert 1.5 galaxy (Markarian et al. 1983; Martel & Osterbrock 1994). The narrow-line spectrum, however, has very weak [N II] lines ( $\lambda 6583/H\alpha = 0.25$ ; Martel & Osterbrock); this is confirmed by our spectra, with even weaker [N II] lines ( $\lambda 6583/H\alpha = 0.10$ ). This object belongs to the class of AGNs with very weak [N II] lines discussed in Sect. 4.3. The individual components used to fit the red spectrum of this object are plotted in Fig. 1.

**NGC 3994** is an Sbc galaxy (Sandage & Bedke 1994) in a triple system, interacting both with NGC 3991 and NGC 3995. Based on the observed line ratios, Keel et al. (1985) classified it as a Liner; the  $\lambda 5007/H\beta$  and  $\lambda 6583/H\alpha$  values rather suggest a H II region. We found that its spectrum is “composite”, the main contribution to the Balmer lines coming from a starburst. The relative strength of the [O I] lines is large in the other component ( $\lambda 6300/H\alpha = 0.53$ ), suggesting that it is a Liner.

**NGC 4102** is a Sb galaxy (Sandage & Bedke 1994). For Ho et al. (1997a) it is a H II region, although its UV spectrum does not resemble that of a starburst galaxy (Kinney et al. 1993). The spectrum published by Ho et al. (1995) rather indicates a “transition object”. Our blue spectrum shows a  $H\beta$  line obviously narrower than the [O III] lines, indicating that the spectrum is “composite”. The blue spectrum was fitted with two sets of three Gaussians. The broadest  $H\beta$  profile in the fit contains 7% of the total  $H\beta$  flux. The red spectrum having a very high signal-to-noise ratio, we needed three sets of three Gaussians to get a good fit; we forced one set to have the same width as the broadest set in the blue fit. The fitting analysis gives two strong narrow components and a weak broad one, containing  $\sim 5\%$  of the total  $H\alpha$  flux and having  $\lambda 6583/H\alpha = 1.57$ . There was no need to use two narrow components to fit the  $H\beta$  line, as the spectrum was taken under poor transparency conditions and its signal-to-noise ratio is much lower. Our conclusion is that the nucleus of NGC 4102 is dominated by a starburst, but that a weak Seyfert 2 component is present and detected mainly by the broadening of the [O III] lines.

**IRAS 12474+4345 S.** For de Grijp et al. (1992), this object is a H II region; however, the published  $\lambda 5007/H\beta$  line ratio (2.93) is slightly high for the corresponding  $\lambda 6583/H\alpha$  ratio (0.42). Fitting our spectra with a single set of lines gives an unsatisfactory result, while the solution with two sets of lines is acceptable, with small residuals. One set of lines corresponds to a H II region, while the other has  $\lambda 5007/H\beta = 4.43$ ,

$\lambda 6300/H\alpha = 0.03$  and  $\lambda 6583/H\alpha = 0.40$ ; these values are intermediate between those corresponding to H II regions and Seyfert 2 nebulosities. Moreover, the He II  $\lambda 4686$  line is detected with  $\lambda 4686/H\beta = 0.17$ , if all the He II flux is attributed to the “transition” component. We are unable to conclude concerning the nature of this second component.

**UGC 8621** is a Seyfert 1.8 galaxy according to Osterbrock & Martel (1993). Our blue spectrum shows the H $\beta$  line to be much narrower ( $< 80 \text{ km s}^{-1}$ ) than the [O III] lines ( $\sim 665 \text{ km s}^{-1}$ ), but no evidence of a broad component. To account for the different widths observed, we fitted the blue spectrum with two sets of lines; for the narrow component, we found  $\lambda 5007/H\beta = 0.28$ , while we have forced the broader component to have  $\lambda 5007/H\beta = 10$ . We fitted the red spectrum with two sets of three Gaussians, imposing to one of them to have the same width as the broader [O III] component; an additional Gaussian was added to fit the broad H $\alpha$  wings. We find no trace of [O I] emission ( $\lambda 6300/H\alpha \leq 0.01$ ) for the narrow component and  $\lambda 6300/H\alpha < 0.3$  for the Seyfert cloud. This is a “composite object”, with a relatively strong H II region and a weak Seyfert 1.9 nebulosity.

**Mark 266** is a merging system with two nuclei separated by  $10''$  (Hutchings & Neff 1988; Wang et al. 1997). It is a Luminous Infrared Galaxy (LIG), i.e.,  $10^{11.2} < L_{\text{IR}} < 10^{12} L_{\odot}$  (Goldader et al. 1997). Line intensity ratios in the two nuclei have been measured by Osterbrock & Dahari (1983), Veilleux & Osterbrock (1987), Mazzarella & Boroson (1993), Osterbrock & Martel (1993) and Kim et al. (1995); all these measurements are in good agreement, if we make the assumption that Kim et al. have inverted the NE and SW components. On the basis of these line ratios, Mark 266 SW has been classified as a Seyfert 2 by Mazzarella & Boroson, Kim et al. and Wu et al. (1998b), and as a “marginal” Seyfert 2 by Osterbrock & Dahari, while Mark 266 NE has been called a Liner by Mazzarella & Boroson, Kim et al. and Wu et al., and a “narrow emission-line galaxy” (NELG) by Osterbrock & Dahari and Veilleux & Osterbrock. NELGs, for these authors, are emission-line galaxies that may be either Liners or H II regions. For Mark 266 NE, we have only a blue spectrum which, by simple visual inspection, shows quite different H $\beta$  and [O III] line profiles. Our line profile analysis reveals two clouds, one with narrow lines (FWHM  $\sim 300 \text{ km s}^{-1}$ ) and  $\lambda 5007/H\beta = 0.96$ , the other with broader lines (FWHM  $\sim 1000 \text{ km s}^{-1}$ ) and  $\lambda 5007/H\beta = 2.2$  and containing 37% of the total H $\beta$  flux. The published value of the intensity ratio  $\lambda 6300/H\alpha$  is 0.15. If the narrow component is associated with a H II region, it contributes in a small amount to the observed [O I] $\lambda 6300$  flux and therefore the  $\lambda 6300/H\alpha$  ratio for the broader component is likely to be significantly larger than 0.12, which means that this component could be a Liner. We have fitted the blue spectrum of Mark 266 SW with three sets of Gaussians: one of them corresponds, most probably, to a H II region with narrow lines ( $295 \text{ km s}^{-1}$  FWHM) and  $\lambda 5007/H\beta = 0.36$ ; the two other sets have widths of 200 and  $600 \text{ km s}^{-1}$  and  $\lambda 5007/H\beta = 3.7$  and 13.3, respectively. We also fitted the red spectrum with three sets of Gaussians, forcing, in addition, one of the sets to have a width of  $600 \text{ km s}^{-1}$ .

The result is a set of narrow lines with  $\lambda 6583/H\alpha = 0.58$  corresponding to the narrow blue lines, confirming that this system is indeed coming from a H II region. The set having the broadest lines has intensity ratios typical of a Seyfert cloud. The third set, with  $\lambda 5007/H\beta = 3.65$  and  $\lambda 6583/H\alpha = 0.58$ , has still an intermediate spectrum.

**Mark 1361** was called a Seyfert 2 galaxy by Kim et al. (1995). Our analysis of a red spectrum (Paper I) led to the conclusion that it is a “composite object”. Our blue spectrum confirms this result. Three sets of three components were needed to get a good fit. In one set we had to impose  $\lambda 5007/H\beta = 10$ , in another  $\lambda 5007/H\beta = 0.1$ . The best fit resulted in a narrow set of lines with very weak [O III] lines and two sets of lines with strong [O III] contribution. We then re-analyzed the red spectrum using three sets of three lines; we had to add a weak broad H $\alpha$  component (FWHM  $\sim 2400 \text{ km s}^{-1}$ , with  $\sim 10\%$  of the total H $\alpha$  flux) in order to obtain a good fit. For the narrowest set of three lines, we found  $\lambda 6583/H\alpha = 0.54$ , for the other two, 0.66 and 1.04 respectively. The conclusion is that Mark 1361 has a “composite” spectrum with a H II cloud contributing half of the H $\beta$  line and a Seyfert 2 nebulosity with complex line profiles (two Gaussians were needed for the fit). If the presence of the broad H $\alpha$  component is confirmed, this object could be a Seyfert 1.9 galaxy.

**Mark 461** is a Seyfert 2 galaxy according to Huchra & Burg (1992); however, Cruz-Gonzalez et al. (1994) have measured  $\lambda 5007/H\beta = 1.13$ . The emission is concentrated in the nuclear region (Gonzalez Delgado et al. 1997). No other line ratios have been published for this object. The H $\beta$  and [O III] lines obviously do not have the same profile. To get a good fit, two sets of lines were necessary. The object is “composite”, one component being a H II region and the other probably a Seyfert 2 nucleus.

**4C 26.42.** This object has been identified with a cD galaxy, MCG 05.33.005 (Carswell & Wills 1967; Olsen 1970; Merckelijn 1972), the brightest member of Abell 1975 (Parma et al. 1986; Pilkington 1964); it is a FR I, Z-shaped radio source (van Breugel et al. 1984; Ge & Owen 1993). Emission lines have been detected in the nuclear region, with  $\lambda 5007/H\beta = 0.4$ ,  $\lambda 6583/H\alpha = 0.8$  and  $\lambda 6300/H\alpha = 0.2$  (Anton 1993). These values are similar to the ones usually observed in Liners, but for the low [O III] $\lambda 5007$  line intensity. Examination of the red spectrum shows that the lines are obviously double. Fitting the lines with two sets of components revealed two clouds with a velocity difference of  $\sim 330 \text{ km s}^{-1}$ . Their line ratios are very similar and typical of Liners with exceptionally weak [O III] lines.

**I Zw 81.** Koski (1978) observed narrow (FWHM =  $225 \pm 200 \text{ km s}^{-1}$ ) emission lines in this galaxy, with  $\lambda 5007/H\beta = 3.14$ ,  $\lambda 6583/H\alpha = 0.67$  and  $\lambda 6300/H\alpha = 0.07$ ; the narrowness of the emission lines and the relative weakness of the [O III] lines led him to conclude that this is not a Seyfert galaxy, but rather a “transition” case between a H II galaxy and a Seyfert 2. Shuder & Osterbrock (1981) and Veilleux & Osterbrock (1987) called it a narrow-line Seyfert. Our red spectrum shows the lines to be double with a separation of  $220 \text{ km s}^{-1}$ . Fitting both



the red and blue spectra with two sets of three Gaussians, we found  $\lambda 5007/\text{H}\beta = 2.05$  (1.41) and  $\lambda 6583/\text{H}\alpha = 0.78$  (0.56) for the high (low) velocity clouds. In both cases, the [O I] lines are undetected with  $\lambda 6300/\text{H}\alpha < 0.04$ . The two clouds are most probably H II regions.

**Mark 477.** This object was discussed in Paper I, where we concluded from the published data and the analysis of a red spectrum that its nature was unclear. Heckman et al. (1997) have argued that the observed UV through near-IR continuum in the nucleus of Mark 477 is dominated by light from a starburst. The narrow Balmer emission lines would then be excited by ionizing radiation from both the hidden Seyfert 1 nucleus and from the hot stars in the starburst. We have re-analyzed our old red spectrum together with our new blue spectrum. Three sets of components were needed to fit these very high signal-to-noise data. The three line-systems are typical of Seyfert 2s, although two have relatively weak [N II] intensities, with  $\lambda 6583/\text{H}\alpha = 0.31$  and  $0.38$ , respectively. We found no evidence for the presence of broad Balmer components.

**Mark 848 S** is a LIG (Goldader et al. 1997) belonging to a pair of interacting galaxies (Armus et al. 1990). The northern galaxy is a H II region (Wu et al. 1998a,b); the southern component has been called a Liner (Mazzarella & Boroson 1993; Veilleux et al. 1995), though its line ratios (Kim et al. 1995) are ambiguous, the [O I] $\lambda 6300$  line being rather weak for a Liner. The line profile analysis of our spectra shows it to be a “composite object” with two distinct emission-line clouds: a narrow one (FWHM  $\sim 140 \text{ km s}^{-1}$ , with  $\lambda 5007/\text{H}\beta = 0.83$ ,  $\lambda 6583/\text{H}\alpha = 0.43$  and  $\lambda 6300/\text{H}\alpha = 0.03$ ), identified with a H II region, and a somewhat broader one (FWHM  $\sim 580 \text{ km s}^{-1}$ ), with line ratios typical of a Seyfert 2 ( $\lambda 5007/\text{H}\beta = 4.20$ ,  $\lambda 6583/\text{H}\alpha = 0.71$  and  $\lambda 6300/\text{H}\alpha = 0.14$ ).

**IRAS 15184+0834.** De Grijp et al. (1992) called this object a Seyfert 2; however they found relatively weak [N II] lines ( $\lambda 6583/\text{H}\alpha = 0.42$ ). Our spectra show that the [N II] lines are significantly stronger than the published values. A reasonable fit is obtained with two sets of components: one is a H II region; the other could be a Seyfert 2, although the [O I] lines are relatively weak.

**NGC 5953** is a peculiar S0 (Rampazzo et al. 1995) or Sa (Delgado & Perez 1996) galaxy interacting with NGC 5954 (Arp 1966). It has a Seyfert 2 nucleus (Rafanelli et al. 1990; Delgado & Perez) surrounded by a ring of star formation with a radius of  $\sim 4''$  (Delgado & Perez). Rafanelli et al. and Delgado & Perez studied this object using a slit width of  $2''.0$  and  $1''.5$  respectively. The seeing was  $\sim 1''$  during Delgado & Perez’ observations, while it was not specified by Rafanelli et al. who, however, easily separated the galaxy nucleus from a star located  $3''$  away. We may reasonably assume that, in both cases, the nuclear spectrum corresponds to a  $2''.0 \times 2''.0$ , or smaller, aperture. The line ratios given by these authors (see Table 2) are typical of a Seyfert 2 region, although [O I] $\lambda 6300$  may be somewhat weak for this type of objects; but as stressed before, we cannot exclude some contamination by the circumstellar emission region. Both Keel et al. (1985) and Kim et al. (1995) have observed the NGC 5953 nuclear region with

a relatively large aperture: Keel et al. used a  $\phi = 4''.7$  circular aperture, while Kim et al. used a long  $2'' \times 14''$  slit. It is clear that these two large aperture spectra must contain a significant contribution from the circumstellar emission region and, indeed, the published line intensity ratios are those of “transition” spectra. We used a  $2''.1$  slit and the seeing was  $2''.6$ ; we extracted 7 columns, i.e.,  $7''.6$ , so some contamination from the circumstellar emission region was expected. Effectively, by doing the line profile fitting analysis, we were able to identify two components of different line widths and strengths, one of which can be associated with a H II region ( $\lambda 5007/\text{H}\beta = 0.55$ ,  $\lambda 6583/\text{H}\alpha = 0.60$ ,  $\lambda 6300/\text{H}\alpha = 0.03$  and FWHM  $\sim 200 \text{ km s}^{-1}$ ); the other component, broader (FWHM  $\sim 400 \text{ km s}^{-1}$ ), reveals the presence of a Seyfert 2 nebula, the measured line intensities being:  $\lambda 6583/\text{H}\alpha = 1.96$  and  $\lambda 6300/\text{H}\alpha = 0.18$ , with  $\lambda 5007/\text{H}\beta$  fixed to 10. Lines of [Fe III] $\lambda 4659$  and [Fe VII] $\lambda 5158$  are clearly visible in the blue spectrum. A very weak broad H $\alpha$  line is possibly detected, which would qualify NGC 5953 as a Seyfert 1.9 galaxy.

**Kaz 49** has been classified as a Seyfert 1 by Yegiazarian & Khachikian (1988), as a Seyfert 1.9 by Moran et al. (1994), who have detected a weak broad H $\alpha$  component (FWHM =  $1\ 150 \text{ km s}^{-1}$ ), and as a H II region by Boller et al. (1994). The latter classification was based on measured line ratios ( $\lambda 5007/\text{H}\beta = 2.58$ ,  $\lambda 6583/\text{H}\alpha = 0.56$ ,  $\lambda 6300/\text{H}\alpha = 0.025$ ) that rather point to a “transition” spectrum. The line profile analysis of our spectra shows a strong H II region ( $\lambda 5007/\text{H}\beta = 2.21$ ,  $\lambda 6300/\text{H}\alpha = 0.05$ ,  $\lambda 6583/\text{H}\alpha = 0.55$ ) and a weak Seyfert 2 component for which we have fixed  $\lambda 5007/\text{H}\beta = 10$ . There is no evidence for the presence of a broad H $\alpha$  component; however, the blended weak H $\alpha$  and [N II] components, each having a FWHM  $\sim 880 \text{ km s}^{-1}$  may be easily mistaken for a broad H $\alpha$  line.

**IRAS 16129-0753** has been classified as a possible Liner by de Grijp et al. (1992) on the basis of the measured line intensity ratios ( $\lambda 5007/\text{H}\beta = 2.03$ ,  $\lambda 6583/\text{H}\alpha = 0.64$ ), although [O I] $\lambda 6300$  was very weak. The line fitting analysis of our blue spectrum shows this object to be “composite”. The red spectrum, which has a relatively low signal-to-noise ratio, is well fitted by a single set of lines corresponding to the H II region; the Seyfert component is undetected.

**IRAS 16382-0613** has been called a Seyfert 2 by Aguero et al. (1995) and a possible Seyfert 2 by de Grijp et al. (1992); however, the [O I] $\lambda 6300$  line is marginally weak for a Seyfert 2, with  $\lambda 6300/\text{H}\alpha = 0.09$  (Aguero et al.). The line profiles on the blue spectrum are obviously complex. Fitting these lines with two sets of Gaussians reveals a narrow component (FWHM  $\sim 350 \text{ km s}^{-1}$ ) with  $\lambda 5007/\text{H}\beta = 3.94$ , and a broader component (FWHM  $\sim 1\ 160 \text{ km s}^{-1}$ ) with  $\lambda 5007/\text{H}\beta = 4.06$ . The red spectrum fit gives a solution compatible with the blue solution plus a broad Balmer line (FWHM  $\sim 5\ 000 \text{ km s}^{-1}$ ). The two components have strong [N II] lines, but the [O I] lines are weak. For the broadest set of lines, we find  $\lambda 6300/\text{H}\alpha < 0.12$ , compatible with a Seyfert 2 nebula; however, the narrow component has  $\lambda 6300/\text{H}\alpha < 0.03$  and seems therefore to have a genuine “transition” spectrum.

**Mark 700** was called a Seyfert 1 galaxy by Denisjuk et al. (1976), who found a broad  $H\alpha$  component. For Koski (1978), it is a weak-lined Seyfert galaxy with Balmer absorption lines, very similar to “normal” emission-line galaxies. Ferland & Netzer (1983) included it in a Liner list, on the basis of the intensity ratios published by Koski. Our observations show that this object is, indeed, a Liner; the broad  $H\alpha$  component seen by Denisjuk et al. is confirmed.

**MCG 03.45.003.** The [N II] lines measured by de Grijp et al. (1992) are rather weak for a Seyfert 2 galaxy ( $\lambda 6583/H\alpha = 0.42$ ) and, on the basis of a red spectrum, we concluded in Paper I that this object could have a “composite” spectrum. Our analysis of both the blue and red spectra show that two kinematically distinct clouds are present in this object, both of them having Seyfert 2 characteristics.

**PGC 61548.** The red spectrum is “composite” and confirms the result presented in Paper I. The line profile analysis reveals the presence of both a H II region ( $\lambda 5007/H\beta = 0.41$ ,  $\lambda 6583/H\alpha = 0.50$ ,  $\lambda 6300/H\alpha = 0.04$ , FWHM  $\sim 250 \text{ km s}^{-1}$ ) and a Seyfert 2 nebulosity ( $\lambda 5007/H\beta$  fixed to 10.0,  $\lambda 6583/H\alpha \sim 3.9$ ,  $\lambda 6300/H\alpha \sim 0.5$  and FWHM  $\sim 570 \text{ km s}^{-1}$ ).

**Kaz 214** is a Seyfert 2 galaxy for de Grijp et al. (1992), with  $\lambda 5007/H\beta = 5.23$  and  $\lambda 6583/H\alpha = 0.39$ ; however, the [N II] lines are weak for a Seyfert 2. On our red exposure, the slit position angle was  $PA = 139^\circ$ . By simple visual inspection of the CCD image, we see that the lines are double: in one of the line-systems the lines are spatially extended and narrow, with relatively weak [N II]; in the other, the lines are spatially unresolved, but relatively broad, and [N II] is stronger. The spectrum is obviously “composite” with a H II region and a Seyfert component. However, when analysing the spectrum obtained by extracting three columns centered on the nucleus, we were unable to get a satisfactory fit confirming the visual impression. We then extracted individually seven columns (numbered 1 to 7, from SE to NW) containing obvious emission lines; the continuum was brightest in columns 4 and 5. Columns 1, 2 and 7 were fitted with a single set of lines, while for columns 3 to 6, two sets of lines were necessary. We have made the assumption that the Seyfert component is really spatially unresolved and, consequently, forced the redshift, width and the  $\lambda 6583/H\alpha$  ratio of this component to be the same on all columns (that is,  $120 \text{ km s}^{-1}$ ,  $525 \text{ km s}^{-1}$  FWHM and 0.60, respectively), the only free parameter being the  $H\alpha$  intensity. In addition to this Seyfert component, we have found, on all columns, a narrow component with relatively weak [N II] lines; the velocity of this narrow component increases from  $-25 \text{ km s}^{-1}$  to  $140 \text{ km s}^{-1}$  from column 1 to 7. The blue spectrum was taken with the slit oriented N-S. As the seeing was rather poor, seven columns were added together when extracting the spectrum. The best fit was obtained with three sets of lines: for one of them, we forced  $\lambda 5007/H\beta = 10$  (this turns to be the broadest component); the two other sets have narrow lines, with moderate  $\lambda 5007/H\beta$  ratios. We therefore conclude that Kaz 214 has a “composite” spectrum. But this example shows that it may not be possible to show that a “transition” spectrum is a “composite” spectrum when the spatial resolution is insufficient, this being due to the

large velocity dispersion gradient sometimes present in the nuclear region which broadens the lines.

**NGC 6764** has been called a Seyfert 2 galaxy by Rubin et al. (1975), in spite of  $H\beta$  being stronger than [O III] $\lambda 5007$ ; this classification was based on the width of the  $H\alpha$  and [N II] lines ( $\sim 750 \text{ km s}^{-1}$ ) but Wilson & Nath (1990) found these lines to be much narrower ( $\sim 380 \text{ km s}^{-1}$  FWHM). Koski (1978) noticed the presence of weak H I absorption lines and, from the line intensity ratios, concluded that it was very much like “normal” galaxies, while for Shuder & Osterbrock (1981), it is not a Seyfert 2. Using the line ratios published by Koski (1978), Ferland & Netzer (1983) classified it as a Liner. Osterbrock & Cohen (1982) have detected in the spectra of this object the  $\lambda 4650$  Wolf-Rayet emission feature. For Ashby et al. (1992), it is a starburst galaxy. Line profile fitting of our spectra revealed the “composite” nature of this object. Two systems were identified: a narrow one (FWHM =  $325 \text{ km s}^{-1}$ ) with line ratios compatible with those usually observed in H II regions ( $\lambda 5007/H\beta = 0.62$ ,  $\lambda 6583/H\alpha = 0.65$  and  $\lambda 6300/H\alpha = 0.04$ ) and a broader system (FWHM =  $480 \text{ km s}^{-1}$ ) with line ratios similar to those of Liners ( $\lambda 5007/H\beta = 0.44$ ,  $\lambda 6583/H\alpha = 0.96$  and  $\lambda 6300/H\alpha = 0.14$ ). This is, therefore, a “composite object”.

**IRAS 22114-1109** was classified a Seyfert 2 by Veilleux et al. (1995); however, the [O III] lines are relatively weak for this type of objects ( $\lambda 5007/H\beta = 4.22$ ; Kim et al. 1995). A line profile analysis was performed on the red and blue spectra. The measured line intensities and widths are compatible with the simultaneous presence on the slit of both a H II region ( $\lambda 5007/H\beta = 1.33$ ,  $\lambda 6583/H\alpha = 0.70$ ,  $\lambda 6300/H\alpha < 0.07$  and FWHM =  $185 \text{ km s}^{-1}$ ) and a Seyfert 2 nebulosity ( $\lambda 5007/H\beta$  fixed to 10.0,  $\lambda 6583/H\alpha = 0.60$ ,  $\lambda 6300/H\alpha = 0.12$  and FWHM =  $415 \text{ km s}^{-1}$ ), so this is another example of a “composite-spectrum object”.

**Mark 308** was called a Seyfert 2 galaxy by Popov & Khachikian (1980) and Zamorano et al. (1994); Véron-Cetty & Véron (1986a) classified it as a H II region, although the published line ratios (Table 2) are unlikely for either classes. The analysis of our blue spectrum (Paper I) showed this object to be “composite” with one narrow component with weak [O III] lines and two broader components with strong [O III] lines; the analysis of our red spectrum confirms this result, the narrow system (FWHM  $\sim 155 \text{ km s}^{-1}$ ) being typical of a H II region (with  $\lambda 5007/H\beta$  fixed to 0.1,  $\lambda 6583/H\alpha = 0.30$  and  $\lambda 6300/H\alpha = 0.06$ ) and the two broader line-sets (FWHMs  $\sim 325$  and  $1045 \text{ km s}^{-1}$ , respectively) of Seyfert-like clouds. Moreover, we have detected a weak broad ( $1725 \text{ km s}^{-1}$  FWHM)  $H\alpha$  component containing  $\sim 7\%$  of the total  $H\alpha$  flux. The companion galaxy, KUG 2239+200 A, at  $z = 0.024$  (Keel & van Soest 1992) and located  $53''$  NE of Mark 308, has a H II-like emission-line spectrum.

**Mark 522** is a Seyfert 2 galaxy according to Veilleux & Osterbrock (1987); however, the [O III] and [O I] lines are relatively weak ( $\lambda 5007/H\beta = 3.23$ ,  $\lambda 6300/H\alpha = 0.07$ ). Our observations show this object to be “composite”, with two different line systems: one, “narrow” (FWHM  $\sim 100 \text{ km s}^{-1}$ ),

typical of a H II region ( $\lambda 5007/\text{H}\beta = 0.63$ ,  $\lambda 6583/\text{H}\alpha = 0.53$  and  $\lambda 6300/\text{H}\alpha < 0.04$ ), the other, somewhat broader (FWHM  $\sim 240 \text{ km s}^{-1}$ ), associated with a Seyfert 2 nebulosity ( $\lambda 5007/\text{H}\beta = 7.87$ ,  $\lambda 6583/\text{H}\alpha = 1.50$  and  $\lambda 6300/\text{H}\alpha < 0.2$ ).

**Mark 313** is a Seyfert 2 galaxy according to Osterbrock & Pogge (1987) (with  $\lambda 5007/\text{H}\beta = 3.52$ ,  $\lambda 6583/\text{H}\alpha = 0.52$  and  $\lambda 6300/\text{H}\alpha = 0.10$ ), and Moran et al. (1996); the [O III] lines are relatively weak for a Seyfert 2. Images in [O III] and  $\text{H}\alpha + [\text{N II}]$  show a very complex structure, with high excitation gas restricted to a symmetric, linear feature (Mulchaey et al. 1996). From a two-component Gaussian fitting of high-dispersion spectra of the nucleus of this object, Maehara & Noguchi (1988) concluded that it is a “composite object” with a H II region and a Liner nebulosity. Line profile analysis of our spectra reveals the contribution of two different line-emitting regions: one, with  $\lambda 5007/\text{H}\beta = 2.29$ ,  $\lambda 6583/\text{H}\alpha = 0.44$ ,  $\lambda 6300/\text{H}\alpha = 0.10$  and narrow width ( $135 \text{ km s}^{-1}$  FWHM), is typical of a H II region; the other, much weaker, is not detected in the blue and its line ratios are  $\lambda 6583/\text{H}\alpha = 0.71$  and  $\lambda 6300/\text{H}\alpha = 0.28$ ; it could be either a Seyfert 2 or a Liner, depending on the  $\lambda 5007/\text{H}\beta$  ratio.

**Zw 453.062** is a LIG (Goldader et al. 1997); it was called a Liner by Veilleux et al. (1995) on the basis of the measured emission line ratios, while Wu et al. (1998a,b) found its properties to be intermediate between H II regions and Liners, although the [O I] lines are very weak. Our spectra suggest that it is a “composite object”, one component being a Seyfert 2 nebulosity and the other a H II region.

**IC 5298** is a LIG (Goldader et al. 1997). Wu et al. (1998a,b) found that its properties are intermediate between H II regions and Liners; it was classified as a Seyfert 2 by Veilleux et al. (1995) although the [O I] lines are rather weak ( $\lambda 6300/\text{H}\alpha = 0.05$ ). Our observations suggest that the spectrum is “composite”, being dominated by a H II region.

### 3. Results

In Fig. 3 we have plotted the FWHMs (corrected for the instrumental broadening) of each individual component, i.e. of each set of lines used to fit the blue and red spectra, as listed in Table 6 (cols. 5 and 10, respectively). The good correlation found between the blue and red FWHMs gives confidence in the fitting analysis.

Figure 4 shows the  $\log(\lambda 5007/\text{H}\beta)$  vs.  $\log(\lambda 6583/\text{H}\alpha)$  and  $\log(\lambda 5007/\text{H}\beta)$  vs.  $\log(\lambda 6300/\text{H}\alpha)$  diagrams traditionally used to classify nuclear emission-line regions into H II regions, Liners or Seyfert 2s. We have delimited in the two diagrams three regions, each corresponding to one of these classes. In Figs. 4a and 4b we have plotted all objects for which line ratios are available in the literature and which are unambiguously classified as H II regions (crosses), Seyfert 2s (open circles) or Liners (open squares); we have also plotted the 61 observed objects suspected of having a “transition” spectrum (filled circles): they fall, at least in one of the diagrams, in a “zone of avoidance”, i.e. outside the regions arbitrary assigned to the classical emission-line regions. In figures 4c and 4d, which are

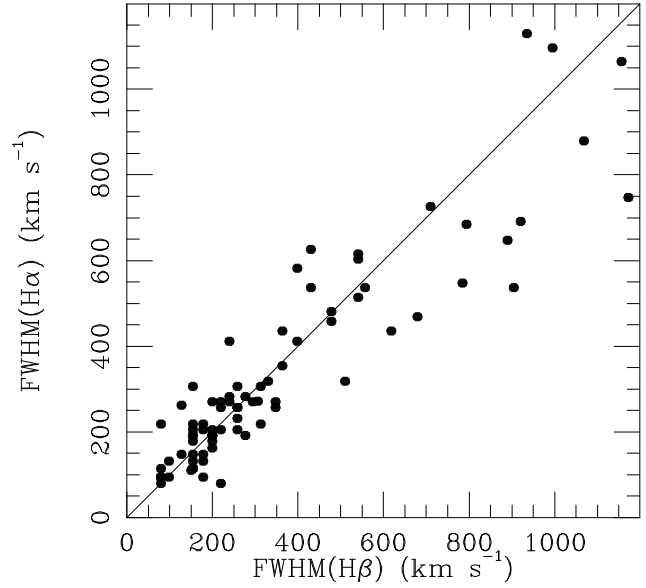


**Fig. 3.** FWHM of all the individual line-components measured on the red spectra vs. the FWHM of the individual components measured on the blue spectra.

the same as 4a and 4b respectively, we have plotted the individual components used to fit the spectra, as given in Table 6.

It is apparent that most of the “transition objects” belong to one of the three following categories:

1. A few objects fall into the “zones of avoidance” only because they have inaccurate published line ratios, appearing to be “normal” when more accurate measurements are obtained; this is the case, for instance, for IRAS 04507+0358, KUG 0825+248, NGC 2989, CG 49 and Arp 107A.
2. A few objects have Seyfert 2 spectra with abnormally weak [N II] lines. They constitute a rare but interesting class of objects which is further discussed below.
3. Most “transition” spectra turn out to be “composite”, due to the simultaneous presence on the slit of a H II region and a Seyfert 2 nebulosity. We have observed 70% of all the objects in an unbiased sample of galaxies displaying a “transition” nuclear spectrum. Modeling of the data revealed that most of them have in fact a “composite” spectrum, suggesting that genuine “transition objects” do not exist at all. However, in a few cases such as NGC 3185, Mark 1291, IRAS 12474+4345S, Mark 266SW or IRAS 15184+0834, we cannot prove that the spectra are “composite”; the classification is ambiguous. Further studies are needed to find out the true nature of these “transition objects”.

Fig. 5 is the histogram of the parameter  $\log(\lambda 6300/\lambda 5007)$  for 159 Seyfert 2s and Liners after correction of the line fluxes for reddening, assuming that the intrinsic Balmer decrement is  $\text{H}\alpha/\text{H}\beta = 3.1$  (Osterbrock & Dahari 1983) [Binette et al. (1990) suggested an even higher value for the intrinsic Balmer decrement in AGNs:  $\text{H}\alpha/\text{H}\beta = 3.4$ ]. The histogram has two main peaks showing a clear separation between strong [O III] $\lambda 5007$

objects (Seyfert 2s) and weak  $[\text{O III}]\lambda 5007$  objects (Liners). Although our sample is heterogeneous and incomplete, this suggests that there is no continuity between the two classes of objects. Heckman (1980) originally defined Liners as objects with  $\lambda 6300/\lambda 5007 > 0.33$ ; it seems that  $\lambda 6300/\lambda 5007 > 0.25$  would be a more realistic definition, as the observed distribution of this ratio really shows a minimum centered around this value.

According to Ho et al. (1997a), the separation between the two principal ionization sources (young stars vs. AGNs) and between the two AGN excitation classes (Seyfert 2 vs. Liners) does not have sharp, rigorously defined boundaries. Fig. 4 shows that this is not the case. In fact, the three areas containing the H II regions, the Seyfert 2s and the Liners are clearly separated; almost every “transition object” turns out to be “composite” when observed with sufficient resolution.

Several authors had already suspected this to be the case. Kennicutt et al. (1989) and Ho et al. (1997c) have shown that the distribution of H II nuclei in the  $\lambda 5007/\text{H}\beta$  vs.  $\lambda 6583/\text{H}\alpha$  plane parallels the disk H II region sequence, the most striking feature being a clear offset between the two classes of objects, the H II nuclei having larger  $\lambda 6583/\text{H}\alpha$  ratios for the same excitation; this effect could be due to the presence of a weak active nucleus in many of these galaxies. Binette (1985) also suggested that mixed cases of starburst and Liner spectra might be relatively common, providing a possible interpretation for objects which have an unusually strong  $\lambda 6300/\text{H}\alpha$  ratio compared to H II regions (NGC 3994, for example). Filippenko & Terlevich (1992) suggested that Liners with weak  $[\text{O I}]$  emission ( $\lambda 6300/\text{H}\alpha < 1/6$ ) might be powered by hot main-sequence stars; however, Ho et al. (1993a) showed that these objects are most probably “composite”.

Ho et al. (1993b) reported the discovery of a non random trend in the dispersion of emission-line intensity ratios for Seyfert 2s.  $\lambda 6300/\text{H}\alpha$  and  $\lambda 6583/\text{H}\alpha$  were found to be correlated with  $\lambda 5007/\text{H}\beta$ , suggesting the influence of a single underlying physical parameter – the hardness of the ionizing continuum. Our data do not show these correlations, which could be artifacts due to the inclusion in the sample of “composite” spectra.

Examination of Fig. 4 shows that the points representative of Seyfert 2 galaxies are not distributed at random in the region assigned to them. Figure 6 is the histogram of the quantity  $\log(\lambda 6583/\text{H}\alpha)$ ; it shows a sharp maximum at  $\sim -0.05$ , with broad wings. Our sample of (131) Seyfert 2 galaxies is not complete in any sense and this could therefore be due to observational biases although this seems unlikely, as the  $\lambda 6583/\text{H}\alpha$  ratio is not used for finding Seyfert 2 galaxies. We have no explanation for this fact.

## 4. Discussion

### 4.1. The blue continuum in Seyfert 2 galaxies

Koski (1978) and Kay (1994) found that all Seyfert 2 galaxies show an ultraviolet excess and weak absorption lines when

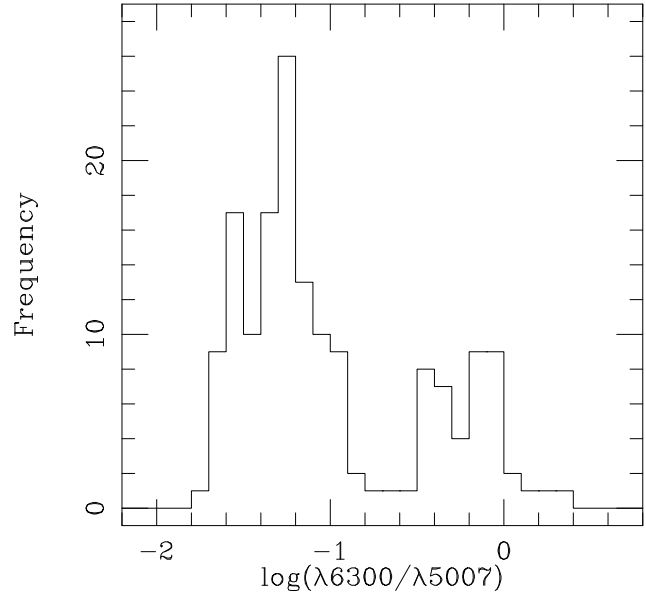


**Fig. 5.** Histogram of  $\log(\lambda 6300/\lambda 5007)$  for the 159 Seyfert 2 and Liners plotted in Fig. 4.

compared with galaxies with no emission lines, indicating the presence of a blue featureless continuum. Boisson & Durret (1986) and Vaceli et al. (1997) suggested that this continuum is a non-thermal power-law continuum. Kinney et al. (1991) argued that most of the Seyfert 2s in which a blue continuum has been observed are of type Sb or earlier, suggesting that it is truly associated with the Seyfert nucleus. Shuder (1981) showed that its strength and the  $\text{H}\alpha$  luminosity are strongly correlated suggesting that a direct physical connection exists between the two; studying a sample of 28 Seyfert 2s, Yee (1980) found that the  $\text{H}\beta$  and continuum fluxes (rather than luminosities) are proportional over two orders of magnitude, with, however, a relatively large dispersion; but a number of those objects are now known to be Seyfert 1 galaxies.

Martin et al. (1983) discovered that a small fraction of all Seyfert 2 galaxies have a highly polarized continuum. Subsequently, Antonucci & Miller (1985), Miller & Goodrich (1990) and Tran et al. (1992) showed that these objects harbour a hidden Seyfert 1 nucleus, the observed polarized continuum arising from scattering of the nuclear continuum by dust or warm electrons. But most Seyfert 2s have very little polarization (Martin et al. 1983), much less than expected in the reflection model (Miller & Goodrich 1990).

On the other hand, Terlevich et al. (1990) showed that in Seyfert 2 galaxies, the IR Ca II triplet is equal or, in some cases, higher than in normal elliptical galaxies, which is most naturally explained by the presence of young stars contributing heavily to the nuclear light at near-IR wavelengths.

Heckman et al. (1995) used *International Ultraviolet Explorer* (IUE) spectra of 20 of the brightest type 2 Seyfert nuclei to build an ultraviolet template for this class; while the continuum was well detected in the template, there was no detectable broad line region (BLR), implying that no more than 20% of

the template continuum could be light from a hidden Seyfert 1 nucleus scattered by dust; they suggested that either most of the nuclei in their sample were “pure” type 2 Seyfert galaxies for which we have a direct view of the central engine and which simply lack of BLR, or that most of the observed ultraviolet continuum is produced by starbursts. From the absence of polarization of the continuum of most Seyfert 2 galaxies and of broad Balmer lines, Cid Fernandez & Terlevich (1995) concluded that, most probably, this continuum was due to a population of young stars in the vicinity of the nucleus. Colina et al. (1997) obtained ultraviolet *HST* images of four nearby Seyfert 2 galaxies known to have circumstellar star-forming rings, providing direct empirical evidence that the UV flux emitted by these galaxies is dominated by radiation coming from clusters of young hot stars distributed along the star-forming ring. If similar rings are a common characteristic of Seyfert 2 galaxies, the large *IUE* aperture would include both the Seyfert 2 nucleus and the rings for distances larger than 25 Mpc. Gonzalez Delgado et al. (1998) presented *HST* images and ultraviolet spectra of three Seyfert 2 nuclei (IC 3639, NGC 5135 and IC 5135); the data show the existence of nuclear starbursts (with absorption features formed in the photosphere of late O and early B stars) dominating the ultraviolet light. It is remarkable that, of the three observed galaxies, two (NGC 5135 and IC 5135) have a “composite” nuclear emission spectrum, while the third (IC 3639), which has the largest UV nuclear flux (associated with the Seyfert nucleus) relative to the total UV flux, has a pure Seyfert 2 spectrum due to the relative weakness of the starburst emission component.

We conclude that there is ample evidence for the presence of young, hot stars in the nuclear region of many Seyfert 2 galaxies. When the continuum is relatively bright, the associated H II region could be strong enough to displace the object into the “transition” zone in the diagnostic diagrams.

AGNs are more frequent in early type galaxies while starbursts are more often found in late-type galaxies (Véron & Véron-Cetty 1986; Ho et al. 1997b; Vaceli et al. 1997). It is therefore rather surprising to find almost systematically a population of young stars in Seyfert 2 galaxies; perhaps the nuclear activity triggers the star formation?

#### 4.2. Excitations and abundances in H II nuclei and AGNs

The  $\lambda 5007/\text{H}\beta$  and  $\lambda 6583/\text{H}\alpha$  ratios are strongly correlated in H II regions. Theoretical studies show that the heavy-metal abundances change continuously along this sequence, a low  $\lambda 5007/\text{H}\beta$  ratio indicating a high metal abundance and a high  $\lambda 5007/\text{H}\beta$  ratio, a low metal abundance, with the heavy metal abundances changing from  $1.5 Z_{\odot}$  at the lower right of Fig. 4a to  $0.25 Z_{\odot}$  at the upper left (see for instance Dopita & Evans 1986; Ho et al. 1997b). However, Stasińska & Leitherer (1996) have shown that most starbursts and H II galaxies can be described as being produced by an evolving starburst with an universal initial mass function embedded in a gas cloud of the same metallicity. The emission line ratios depend mainly on two independent parameters: the age of the starburst and

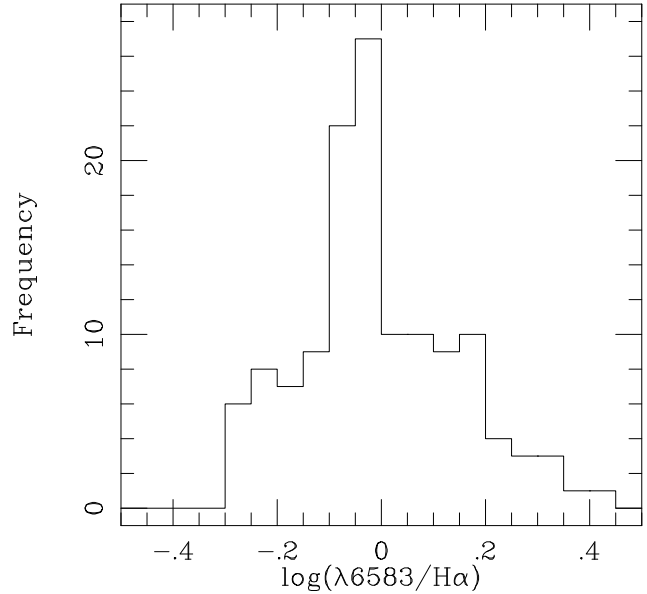


**Fig. 6.** Histogram of  $\log(\lambda 6583/\text{H}\alpha)$  for the 131 Seyfert 2 galaxies plotted in Fig. 4.

the metallicity. In this scenario, the  $\lambda 5007/\text{H}\beta$  ratio effectively changes with these two parameters and therefore is not a direct measurement of metallicity. The metallicity is strongly correlated with luminosity, luminous galaxies having higher metallicities; this correlation is also valid for elliptical galaxies, for which the metallicity is determined from absorption lines with  $[\text{O}/\text{H}] \sim 1$  at  $M_B = -21$  (Salzer et al. 1989; Zaritsky et al. 1994).

AGNs are known to occur preferentially in high luminosity (Ho et al. 1997b), early-type (Véron & Véron-Cetty 1986; Vacali et al. 1997) galaxies; they are therefore expected to have high metallicities. Indeed, the NLRs of active galactic nuclei have enhanced nitrogen abundances (Storchi-Bergmann & Pastoriza 1989, 1990; Storchi-Bergmann et al. 1992; Schmitt et al. 1994). In these NLRs,  $[\text{N}/\text{O}]$  correlates with  $[\text{O}/\text{H}]$  in a manner identical to H II regions in normal galaxies, with nuclear  $[\text{O}/\text{H}]$  and  $[\text{N}/\text{O}]$  values ranging from  $1 Z_{\odot}$  to  $2 Z_{\odot}$  (Storchi-Bergmann et al. 1996b). Storchi-Bergmann et al. (1996b,c) have determined the chemical composition of the H II regions in the ring surrounding the nucleus of several AGNs, as well as in the nuclei; high metallicities were found ( $[\text{O}/\text{H}] \sim 2 Z_{\odot}$  and  $[\text{N}/\text{O}] \sim 3 Z_{\odot}$ ) both in the H II regions and in the AGNs, these abundances being similar to those found in the nuclei of non-active galaxies with the same morphological type and absolute magnitude. Further work by Storchi-Bergmann et al. (1998) has shown that, in fact, oxygen abundances derived for Seyfert 2 nebulosities and neighbouring H II regions (assuming that the emission lines in the active nucleus are due to photoionization by a typical active galactic nucleus continuum) are well correlated, while this is not the case for Liners. This suggests that the gas in AGNs and in the neighbouring H II regions has the same origin and that the scatter observed in the Seyfert 2 region in the diagnostic diagrams, involving the  $\lambda 6583/\text{H}\alpha$  ratio,

is due to variations in the nitrogen abundance. In NGC 6300, in which  $\lambda 6583/\text{H}\alpha = 3.4$ , the nitrogen abundance is estimated to be  $\sim 5 Z_{\odot}$ .

We have seen that nuclear H II regions and Seyfert 2 nebularities, when appearing in the same galaxy, have the same high metallicity; as a result of their metallicity, the H II regions have a low excitation, while the Seyfert 2 nebularities have a high excitation. This explains why it is relatively easy to separate the two components in “transition” spectra.

#### 4.3. Objects with weak [N II] lines

Figure 4 shows a small number of objects which have very weak [N II] lines for Seyfert 2 galaxies; their [O I] lines are however normal for this class of objects.

The first photoionization models invoked to explain the narrow emission lines in AGNs assumed a single density cloud. However, new observations quickly suggested the presence of several emitting clouds, ruling out single component models. Most of the multicloud models first studied were such that the emitting gas, as a whole, was ionization-bounded and thus the He II  $\lambda 4686$  line intensity relative to  $\text{H}\beta$  was determined by the hardness of the ionizing spectrum. In these models, the extreme values reached by the  $\lambda 4686/\text{H}\beta$  ratio are not well reproduced. A number of objects have  $\lambda 4686/\text{H}\beta$  of the order of 0.2 or more; such high values cannot be accounted for unless the line emitting clouds are matter-bounded (Stasińska 1984). On the basis of a weak trend for the low excitation lines to become weaker as  $\lambda 4686/\text{H}\beta$  gets larger, Viegas-Aldrovandi (1988) and Viegas & Prieto (1992) argued in favor of a model in which matter-bounded clouds are present; indeed, if the gas is not optically thick to all the ionizing continuum (i.e., is matter bounded), the  $\text{H}^+$  emitting volume is smaller, but the  $\text{He}^{++}$  volume is not, leading to a higher  $\lambda 4686/\text{H}\beta$  line ratio. Moreover, Viegas-Aldrovandi & Gruenwald (1988) and Rodriguez-Ardila et al. (1998) showed that, for most AGNs, the observed low-excitation lines are better explained by matter-bounded models with about 50% of the  $\text{H}\beta$  luminosity produced in ionization-bounded clouds.

Storchi-Bergmann et al. (1996a) have obtained long-slit spectra of five active galaxies showing extended high excitation lines. At some positions, two of the objects (PKS 0349–27 and PKS 0634–20) show quite peculiar line ratios, with a strong He II  $\lambda 4686$  line ( $\lambda 4686/\text{H}\beta > 0.3$ ) and weak [N II] lines (that is,  $\lambda 6583/\text{H}\alpha < 0.3$ ). In fact, there seems to be a correlation between  $\lambda 6583/\text{H}\alpha$  and  $\lambda 4686/\text{H}\beta$ , weak [N II] lines being associated with strong He II emission, suggesting that very small  $\lambda 6583/\text{H}\alpha$  ratios (as observed in the two above mentioned radiogalaxies) are not necessarily a signature of star-formation, but a natural consequence of having a region dominated by matter-bounded clouds (Binette et al. 1996, 1997). However, in the extranuclear regions of PKS 0349–278 in which strong He II  $\lambda 4686$  and weak [N II]  $\lambda 6583$  lines are observed, the [O I]  $\lambda 6300$  line is also reduced ( $\lambda 6300/\text{H}\alpha \sim 0.05$ ), which is a natural consequence of the model (Viegas-Aldrovandi 1988), while in our sample of weak [N II]  $\lambda 6583$  galaxies, we verify

that the [O I]  $\lambda 6300$  line is not weakened in most of the objects.

In Table 8 we give the list of known AGNs with relatively weak [N II] lines ( $\lambda 6583/\text{H}\alpha < 0.45$ ) with published values of the  $\lambda 4686/\text{H}\beta$  and  $\lambda 6300/\text{H}\alpha$  ratios. Three objects in this table (UM 85, MS 04124–0802 and Mark 699) have both weak [N II] lines ( $\lambda 6583/\text{H}\alpha < 0.20$ ) and a strong He II line ( $\lambda 4686/\text{H}\beta > 0.30$ ). In the last two, the [O I] lines are also relatively weak ( $\lambda 6300/\text{H}\alpha \leq 0.05$ ); these two objects could be dominated by matter-bounded clouds. Alternatively, in the other objects, the weakness of the [N II] lines could be due to a selective under-abundance of nitrogen. For a photoionized single cloud model with  $U \sim 10^{-2.5}$ , Ferland & Netzer (1983) predicted  $\lambda 6583/\text{H}\alpha \sim 1.0$  for solar nitrogen abundances and  $\sim 0.3$  for nitrogen abundances  $\sim 0.3$  solar.

**Table 8.** Known AGNs with weak [N II] lines.

Name	Short position	$\lambda 6583/\text{H}\alpha$	$\lambda 4686/\text{H}\beta$	$\lambda 6300/\text{H}\alpha$
UM 85	01 04+06	0.19	0.37	0.09
MS 04124–0802	04 12–08	0.10	0.35	0.05
IRAS 04210+0400	04 21+04	0.35	0.21	0.13
3C 184.1	07 34+80	0.22	0.26	0.07
IRAS 11058–1131	11 05–11	0.38	0.17	0.05
SBS 1136+594	11 36+59	0.10	0.18	0.11
Mark 477	14 39+53	0.36	0.13	0.17
Mark 699	16 22+41	0.20	0.34	0.03

#### 4.4. Seyfert 2s and Liners

It has been suggested by several authors (see for instance Ferland & Netzer 1983; Shields 1992; Ho et al. 1993a) that in Seyfert 2s, as well as in Liners, the ionized gas is excited by a non-thermal continuum, the only differences being the value of the ionizing parameter which would be  $\sim 10^{-3.5}$  for Liners, and  $\sim 10^{-2.5}$  for Seyfert 2s. If this is the case, the discontinuity between Seyfert 2s and Liners is not easily understood. No reliable detection of the He II line in *bona fide* Liners has been reported suggesting that there could be a serious problem with the picture of simply reducing  $U$  in a standard power-law photoionization model predicting  $\lambda 4686/\text{H}\beta > 0.15$  (Viegas-Aldrovandi & Gruenwald, 1990), as the weakness of He II indicates that the continuum illuminating the NLR clouds must contain few photons more energetic than 54.4 eV, the ionization potential of  $\text{He}^+$  (Péquignot 1984). Binette et al. (1996) proposed that the emission spectrum of Liners is due to ionization-bounded clouds illuminated by a ionization spectrum filtered by matter-bounded clouds hidden from view by obscuring material. In this case, the He II emission is reduced ( $\lambda 4686/\text{H}\beta < 0.01$ ). However, a nearly total obscuration of the matter-bounded component must then be invoked in order to keep the emission from He II at an acceptable low level, a scenario which seems to be rather unlikely to Barth et al. (1996).

## 5. Conclusions

We have shown that:

- Nuclear H II regions, Seyfert 2s and Liners lie in distinct, well separated regions in the  $\log(\lambda 5007/H\beta)$  vs.  $\log(\lambda 6583/H\alpha)$  and  $\log(\lambda 5007/H\beta)$  vs.  $\log(\lambda 6300/H\alpha)$  diagrams. There is no continuity between Liners and Seyfert 2s, with an apparent deficit of objects with  $\lambda 6300/\lambda 5007 = 0.25$ .
- A number of objects have “transition” spectra, falling outside the regions assigned to the three types of emission nebularities. They probably all have a “composite” spectrum.
- We have isolated a class of Seyfert 2 galaxies with weak [N II] lines. This weakness could be due to an under-abundance of nitrogen or to the presence of matter-bounded clouds in these objects.

*Acknowledgements.* This research has made use of the NASA / IPAC extragalactic database (NED) which is operated by the Jet Propulsion Laboratory, Caltech, under contract with the National Aeronautics and Space Administration. A. C. Gonçalves acknowledges support from the *Fundação para a Ciência e a Tecnologia*, Portugal, during the course of this work (PhD. grant ref. PRAXIS XXI/BD/5117/95).

## References

- Afanasjev V.L., Lipovetski V.A., Markarian B. E., Stepanian D. A., 1980, *Astrophys. J.* 16, 119.
- Afanasjev V.L., Lipovetski V. A., Shapovalova A. I., 1981, *Astrophys. J.* 17, 342
- Aguero E. L., Suarez F., Paolantonio S., 1995, *PASP* 107, 959
- Andreassian N., Alloin D., 1994, *A&AS* 107, 23
- Anton K., 1993, *A&A* 270,60
- Antonucci R.R.J., 1985, *ApJS* 59, 459
- Antonucci R.R.J., Miller J.S., 1985, *ApJ* 297, 621
- Armus L., Heckman T.M., Miley G.K., 1990, *ApJ* 364, 471
- Arp H., 1966, *ApJS* 14,1
- Ashby M., Houck J. R., Hacking P. B., 1992, *AJ* 104, 80
- Augarde R., Chalabaev A., Comte G., Kunth D., Maehara H., 1994, *A&AS* 104, 259
- Baldwin J. A., Phillips M. M., Terlevich R., 1981, *PASP* 93, 5
- Barth A.J., Reichert G.A., Filippenko A. V. et al., 1996, *AJ* 112, 1829
- Beichman C., Wynn-Williams C. G., Lonsdale C. J. et al., 1985, *ApJ* 293, 148
- Bica E., 1988, *A&A* 195, 76
- Binette L., 1985, *A&A* 143, 334
- Binette L., Calvet N., Canto J., Raga A.C., 1990, *PASP* 102, 723
- Binette L., Wilson A.S., Storchi-Bergmann T., 1996, *A&A* 312, 365
- Binette L., Wilson A.S., Raga A., Storchi-Bergmann T., 1997, *A&A* 327, 909
- Boisson C., Durret F., 1986, *A&A* 168, 2
- Boller T., Fink H., Schaeidt S., 1994, *A&A* 291, 403
- Boller T., Brandt W.N., Fink H., 1996, *A&A* 305, 53
- Boller T., Bertoldi F., Dennefeld M., Voges W., 1998, *A&AS* 129, 87
- Bowen D.V., Osmer S.J., Blades J.C. et al. 1994, *AJ* 107, 461
- Bower G., Wilson A., Morse J.A. et al., 1995, *ApJ* 454, 106
- Busko I.C., Steiner J.E., 1990, *MNRAS* 245, 470
- Carballo R., Wesselius P. R., Whittet D. C. B., 1992, *A&A* 262,106
- Carswell J. R., Wills D., 1967, *MNRAS* 135, 231
- Cid Fernandez R., Terlevich R., 1995, *MNRAS* 272, 423
- Cohen R.D., Osterbrock D. E., 1981, *ApJ* 243, 81
- Colina L., Garcia-Vargas M.L., Gonzalez Delgado R.M. et al., 1997, *ApJ* 488, L71
- Cruz-Gonzalez I., Carrasco L., Serrano A. et al., 1994, *ApJS* 94, 47
- Dahari O., 1985, *ApJS* 57, 643
- Dahari O., de Robertis M.M., 1988, *ApJS* 67, 249
- de Grijp M.H.K., Miley G.K., Lub J., 1987, *A&AS* 70, 95
- de Grijp M.H.K., Keel W.C., Miley G.K., Goudfrooij P., Lub J., 1992, *A&AS* 96, 389
- de Robertis M.M., Osterbrock D.E., 1986, *ApJ* 301, 727
- Delgado R.M.G., Perez E., 1996, *MNRAS* 281, 781
- Denisjuk E.K., Lipovetski V.A., Afanasjev V.L., 1976, *Astrophys. J.* 12, 442
- Dopita M.A., Evans I.N., 1986, *ApJ* 307, 431
- Duc P.-A., Mirabel I.F., Maza J., 1997, *A&AS* 124, 533
- Ferland G.J., Netzer H., 1983, *ApJ* 264, 105
- Filippenko A.V., Sargent W.L.W., 1985, *ApJS* 57, 503
- Filippenko A.V., Terlevich R., 1992, *ApJ* 397, L79
- Fruscione A., Griffiths R.E., 1991, *ApJ* 380, L13
- Ge J.P., Owen F.N., 1993, *AJ* 105, 778
- Goldader J.D., Joseph R.D., Doyon R., Sanders D.B., 1997, *ApJS* 108, 449
- Gonzalez Delgado R.M., Perez E., Tadhunter C., Vilchez J.M., Rodriguez-Espinoza J.M., 1997, *ApJS* 108, 155
- Gonzalez Delgado R.M., Heckman T., Leitherer C. et al., 1998, *ApJ* 505, 174
- Goodrich R.W., 1989, *ApJ* 342, 224
- Goodrich R.W., Osterbrock D.E., 1983, *ApJ* 269, 416
- Halpern J.P., Oke J.B., 1987, *ApJ* 312, 91
- Haniff C.A., Wilson A.S., Ward M.J., 1988, *ApJ* 334, 104
- Heckman T.M., 1980, *A&A* 87, 152
- Heckman T.M., Miley G.K., van Breugel W.J.M., Butcher H.R. 1981, *ApJ* 247, 403
- Heckman T.M., van Breugel W., Miley G.K., Butcher H.R., 1983, *AJ* 88, 1077
- Heckman T.M., Krolick J., Meurer G. et al., 1995, *ApJ* 452, 549
- Heckman T.M., Gonzalez Delgado R.M., Leitherer C. et al., 1997, *ApJ* 482, 114
- Hill G.J., Wynn-Williams C.G., Becklin E. E., Mackenty J.W., 1988, *ApJ* 335, 93
- Ho L.C., Filippenko A.V., Sargent W.L.W., 1993a, *ApJ* 417, 63
- Ho L.C., Shields J.C., Filippenko A. V., 1993b, *ApJ* 410, 567
- Ho L.C., Filippenko A.V., Sargent W.L.W., 1995, *ApJS* 98, 477
- Ho L.C., Filippenko A.V., Sargent W.L.W., 1997a, *ApJS* 112, 315
- Ho L.C., Filippenko A.V., Sargent W.L.W., 1997b, *ApJ* 487, 568
- Ho L.C., Filippenko A.V., Sargent W.L.W., 1997c, *ApJ* 487, 579
- Holloway A.J., Steffen W., Pedlar A. et al., 1996, *MNRAS* 279, 171
- Holtzman J., Hester J.J., Casertano S. et al. 1995, *PASP* 107, 156
- Huchra J. P., Burg R., 1992, *ApJ* 393, 20
- Hutchings J.B., Neff S.G., 1988, *AJ* 96, 1227
- Kay L.E., 1994, *ApJ* 430, 196
- Kazarian M.A., 1979, *Astrophys. J.* 15, 1
- Keel W.C., 1984, *ApJ* 282, 75
- Keel W.C., 1996, *AJ* 111, 696
- Keel W.C., Kennicutt Jr. R.C., Hummel E., van der Hulst J.M., 1985, *AJ* 90, 708
- Keel W.C., van Soest E.T.M., 1992, *A&AS* 94, 553
- Kennicutt R.C., Keel W.C., Blaha C.A., 1989, *AJ* 97, 1022
- Kim D.-C., Sanders D.B., Veilleux S., Mazzarella J.M., Soifer B.T., 1995, *ApJS* 98, 129
- Kinney A. L., Antonucci R. R. J., Ward M. J., Wilson A. S., Whittle M., 1991, *ApJ* 377, 100

- Kinney A.L., Bohlin R.C., Calzetti D. et al., 1993, *ApJS* 86, 5
- Klaas U., Elsasser H., 1991, *A&AS* 90, 33
- Kollatschny W., Biermann P., Fricke K.J., Huchtmeier W., Witzel A., 1983, *A&A* 119, 80
- Koratkar A., Deustua S.E., Heckman T. et al., 1995, *ApJ* 440, 132
- Koski A.T., 1978, *ApJ* 223, 56
- Lemaître G., Kohler D., Lacroix D., Meunier J.-P., Vin A., 1989, *A&A* 228, 546
- Liu C.T., Kennicutt R.C., 1995, *ApJS* 100, 325
- Maehara H., Noguchi T., 1988, *Ap&SS* 143, 339
- Markarian B. E., Lipovetski V. A., 1971, *Astrophys. J.* 7, 299
- Markarian B. E., Lipovetski V. A., 1973, *Astrophys. J.* 7, 283
- Markarian B. E., Lipovetski V. A., 1974, *Astrophys. J.* 10, 185
- Markarian B. E., Lipovetski V. A., Stepanian D. A., 1979a, *Astrophys. J.* 15, 235
- Markarian B. E., Lipovetski V. A., Stepanian D. A., 1979b, *Astrophys. J.* 15, 363
- Markarian B. E., Stepanian D. A., 1983, *Astrophys. J.* 19, 354
- Martel A., Osterbrock D. E., 1994, *AJ* 107, 1283
- Martin P.G., Thompson I.B., Maza J., Angel J.R.P., 1983, *ApJ* 266, 470
- Massey P., Strobel K., Barnes J.V., Anderson E., 1988, *ApJ* 328, 315
- Mazzarella J. M., Boroson T. A., 1993, *ApJS* 85, 27
- Merkelijn J. K., 1972, *Australian J. Phys.* 25, 451
- Miller J.S., Goodrich R.W., 1990, *ApJ* 355, 456
- Moorwood A. F. M., Véron-Cetty M.-P., Glass I.S. 1986, *A&A* 160, 39
- Moran E. C., Halpern J. P., Helfand D. J., 1994, *ApJ* 433, L65
- Moran E. C., Halpern J. P., Helfand D. J., 1996, *ApJS* 106, 341
- Morgan W.W., 1958, *PASP* 70, 364
- Morgan W.W., 1959, *PASP* 71, 394
- Mulchaey J.S., Wilson A.S., Tsvetanov Z., 1996, *ApJS* 102, 309
- Murphy T. W., Armus L., Matthews K. et al., 1996, *AJ* 111, 1025
- Netzer H., Kollatschny W., Fricke K. J., 1987, *A&A* 171, 41
- Oke J. B., 1974, *ApJS* 27, 21
- Oke J. B., Gunn J. E., 1983, *ApJ* 206, 713
- Olsen E. T., 1970, *AJ* 75, 764
- Osterbrock D. E., 1974, *Astrophysics of gaseous nebulae. Freeman and company, San Francisco*
- Osterbrock D. E., Cohen R. D., 1982, *ApJ* 261, 64
- Osterbrock D. E., Dahari O., 1983, *ApJ* 273, 478
- Osterbrock D. E., de Robertis M. M., 1985, *PASP* 97, 1129
- Osterbrock D. E., Martel A., 1993, *ApJ* 414, 552
- Osterbrock D. E., Pogge R. W., 1987, *ApJ* 323, 108
- Parma P., de Ruiter H. R., Fanti C., Fanti R., 1986, *A&AS* 64, 135
- Péquignot D., 1984, *A&A* 131, 159
- Pesch P. & Sanduleak N., 1983, *ApJS* 51, 171
- Petrosian A. R., Saakian K. A., Khachikian E. E., 1978, *Astrophys. J.* 14, 36
- Petrosian A. R., Saakian K. A., Khachikian E. E. 1979, *Astrophys. J.* 15, 250
- Phillips M. M., Charles P. A., Baldwin J. A., 1983, *ApJ* 266, 485
- Pilkington J. H. D., 1964, *MNRAS* 128, 103
- Popov V. N., Khachikian E. E., 1980, *Astrophys. J.* 16, 33
- Rafanelli P., Osterbrock D. E., Pogge R. W., 1990, *AJ* 99, 53
- Rafanelli P., Marziani P., Birkle K., Thiele U., 1993, *A&A* 275, 451
- Rampazzo R., Reduzzi L., Sulentic J. W., Madejsky R., 1995, *A&AS* 110, 131
- Rodriguez-Ardila A., Pastoriza M.G., Maza J., 1998, *ApJ* 494, 202
- Rubin V. C., Thonnard N., Ford W. K., 1975, *ApJ* 199, 31
- Salzer J.J., MacAlpine G.M., Boroson T.A., 1989, *ApJS* 70, 479
- Salzer J.J., Moody J.W., Rosenberg J.L., Gregory A., Newberry M.V., 1995, *AJ* 109, 2376
- Sandage A., Bedke J., 1994, *The Carnegie atlas of galaxies*
- Sanders D. B., Soifer B. T., Elias J. H. et al., 1988, *ApJ* 325, 74
- Schmitt H.R., Storchi-Bergmann T., Baldwin J.A., 1994, *ApJ* 423, 237
- Shields J.C., 1992, *ApJ* 399, L27
- Shuder J.M., 1981, *ApJ* 244, 12
- Shuder J.M., Osterbrock D.E., 1981, *ApJ* 250, 55
- Stasińska G., 1984, *A&A* 135, 341
- Stasińska G., Leitherer C., 1996, *ApJS* 107, 661
- Stauffer J. R., 1982, *ApJ* 262, 66
- Steffen W., Holloway A.J., Pedlar A., 1996, *MNRAS* 282, 1203
- Stone R. P. S., 1977, *ApJ* 218, 767
- Storchi-Bergmann T., Pastoriza M. G., 1989, *ApJ* 347, 195
- Storchi-Bergmann T., Pastoriza M.G., 1990, *PASP* 102, 1359
- Storchi-Bergmann T., Wilson A.S., Baldwin J.A., 1992, *ApJ* 396, 45
- Storchi-Bergmann T., Wilson A.S., Mulchaey J.S., Binette L., 1996a, *A&A* 312, 357
- Storchi-Bergmann T., Rodriguez-Ardila A., Schmitt H.R. et al., 1996b, *ApJ* 472, 83
- Storchi-Bergmann T., Wilson A.S., Baldwin J.A., 1996c, *ApJ* 460, 252
- Storchi-Bergmann T., Schmitt H.R., Calzetti D., Kinney A.L., 1998, *AJ* 115, 509
- Takase B., Miyauchi-Isobe N., 1986, *Ann. Tokyo Astron. Obs.* 21, 127
- Takase B., Miyauchi-Isobe N., 1990, *Pub. Nat. Obs. Japan* 1, 181
- Terlevich E., Diaz A.I., Terlevich R., 1990, *MNRAS* 242, 271
- Tran H.D., Miller J.S., Kay L.E., 1992, *ApJ* 397, 452
- Trauger J.T., Ballester G.E., Burrows C.J., et al. 1994, *ApJ* 435, L3
- Ulvestad J. S., Wilson A. S., 1983, *AJ* 88, 253
- Vaceli M.S., Viegas S.M., Gruenwald R., de Souza R.E., 1997, *AJ* 114, 1345
- van Breugel W., Heckman T., Miley G., 1984, *ApJ* 276, 79
- Veilleux S., 1991a, *ApJS* 75, 357
- Veilleux S., 1991b, *ApJS* 75, 383
- Veilleux S., 1991c, *ApJ* 369, 331
- Veilleux S., Osterbrock D. E., 1987, *ApJS* 63, 295
- Veilleux S., Kim D.-C., Sanders D. B., Mazzarella J. M., Soifer B. T., 1995, *ApJS* 98, 171
- Véron M.-P., Véron P., Zuiderwijk E. J., 1981b, *A&A* 98, 34
- Véron-Cetty M.-P., Véron P., 1984, *A Catalogue of Quasars and Active Nuclei, ESO Scientific Report No. 1, Garching: European Southern Observatory (ESO)*
- Véron-Cetty M.-P., Véron P., 1985, *A&A* 145, 425
- Véron-Cetty M.-P., Véron P., 1986a, *A&AS* 65, 241
- Véron-Cetty M.-P., Véron P., 1986b, *A&AS* 66, 335
- Véron-Cetty M.-P., Véron P., 1996, *A&AS* 115, 97
- Véron P., Linblad P. O., Zuiderwijk E. J., Véron M.-P., Adam G., 1980, *A&A* 87, 245
- Véron P., Véron-Cetty M.-P., 1986, *A&A* 161, 145
- Véron P., Véron-Cetty M.-P., Bergeron J., Zuiderwijk E. J., 1981b, *A&A* 97, 71
- Véron P., Véron-Cetty M.-P., Zuiderwijk E. J., 1981c, *A&A* 102, 116
- Véron P., Gonçalves A. C., Véron-Cetty M.-P., 1997, *A&A* 319, 52 (Paper I)
- Viegas S.M., Prieto M.A., 1992, *MNRAS* 258, 483
- Viegas-Aldrovandi S.M., 1988, *ApJ* 330, L9
- Viegas-Aldrovandi S.M., Gruenwald R.B., 1988, *ApJ* 324, 683
- Viegas-Aldrovandi S.M., Gruenwald R.B., 1990, *ApJ* 360, 474
- Vogel S., Engels D., Hagen H.-J. et al., 1993, *A&AS* 98, 193
- Wang J., Heckman T. M., Weaver K. A., Armus L., 1997, *ApJ* 474, 659



- Wilson A.S., Nath B., 1990, ApJS 74, 731  
Wu H., Zou Z.L., Xia X.Y., Deng Z.G., 1998a, A&AS 127, 521  
Wu H., Zou Z.L., Xia X.Y., Deng Z.G., 1998b, A&A (in press)  
Wyndham J. D., 1966, ApJ 144, 459  
Yee H.K.C., 1980, ApJ 241, 894  
Yegiazarian A. A., Khachikian E. Y., 1988, Soob. Byu. Spets. Astrofiz.  
Obs. 60, 3  
Zaritsky D., Kennicutt R.C., Huchra J.P. 1994, ApJ 420, 87  
Zamorano J., Rego M., Gallego J. et al., 1994, ApJS 95, 387

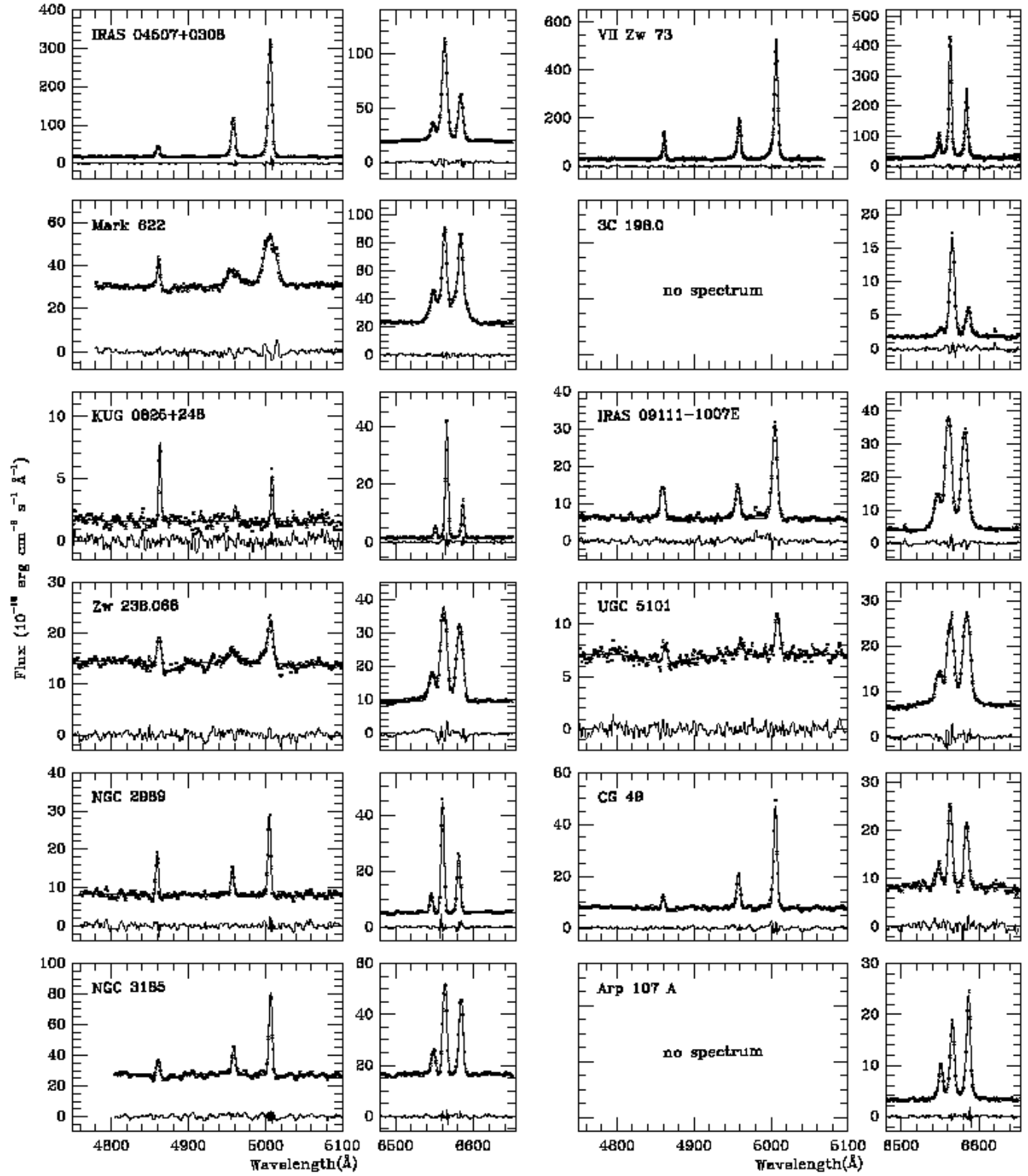


Fig. 1. Blue and red spectra for the 53 galaxies studied in this paper (continued).

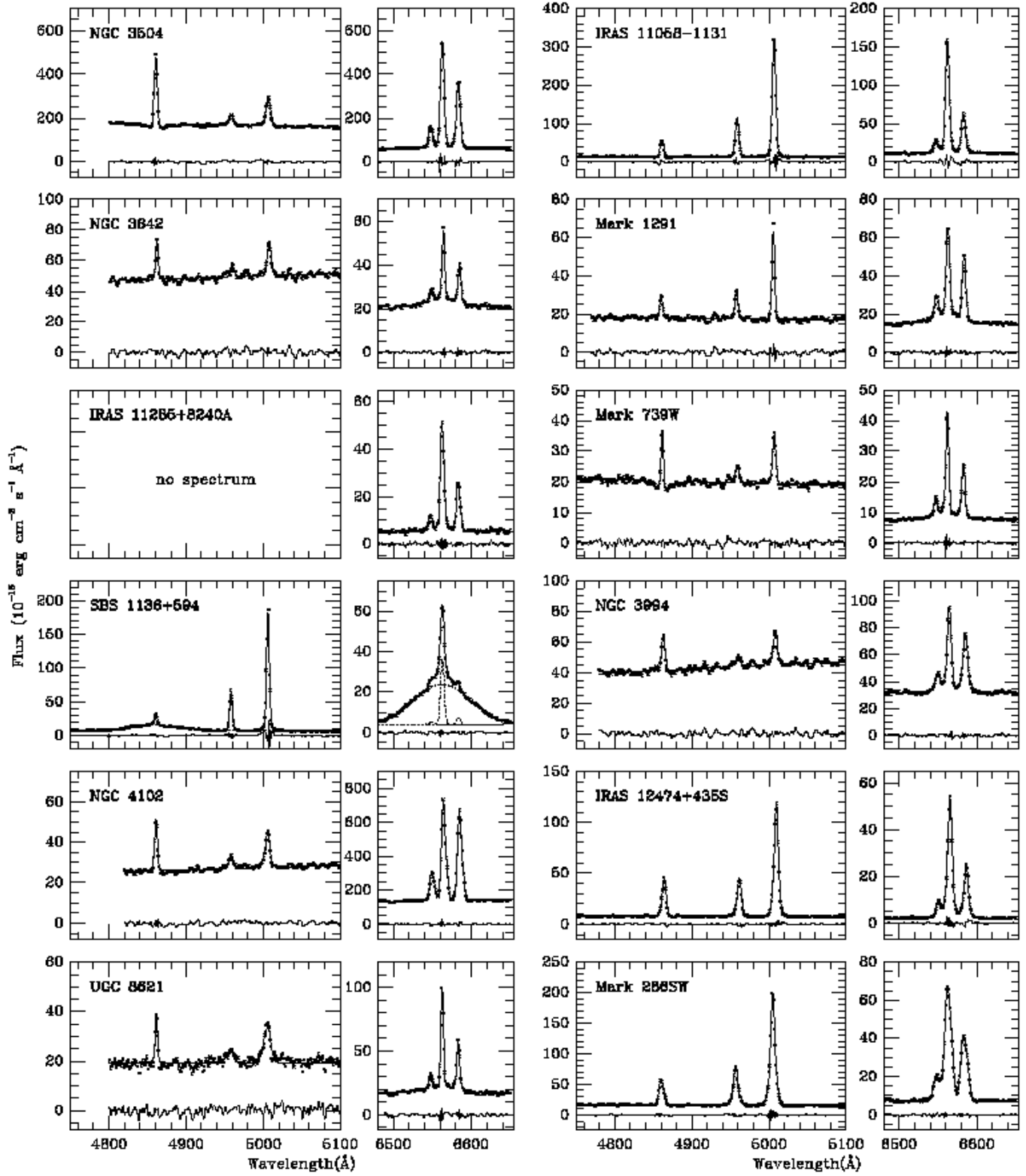


Fig. 1. Blue and red spectra for the 53 galaxies studied in this paper (continued).

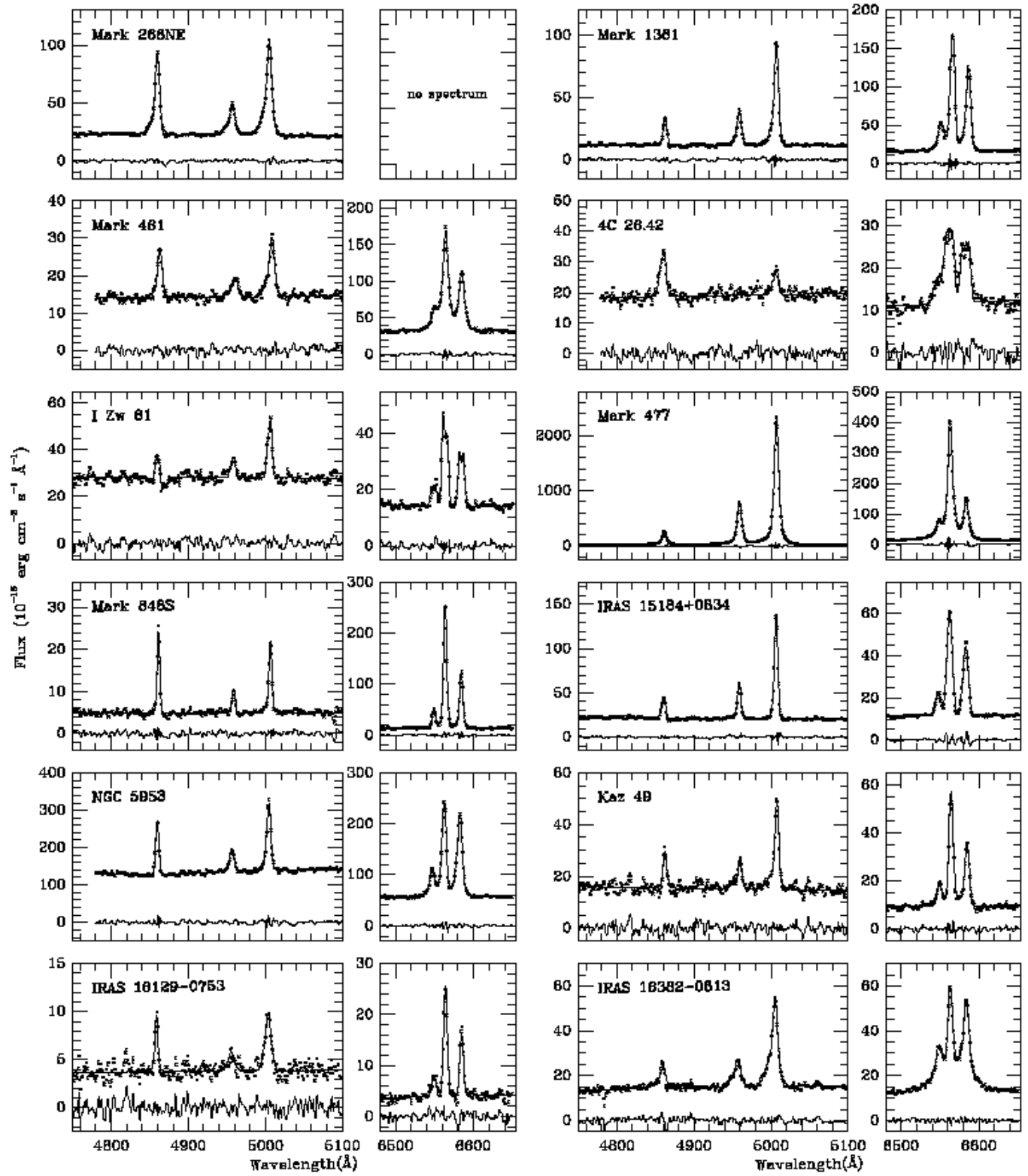


Fig. 1. Blue and red spectra for the 53 galaxies studied in this paper (continued).

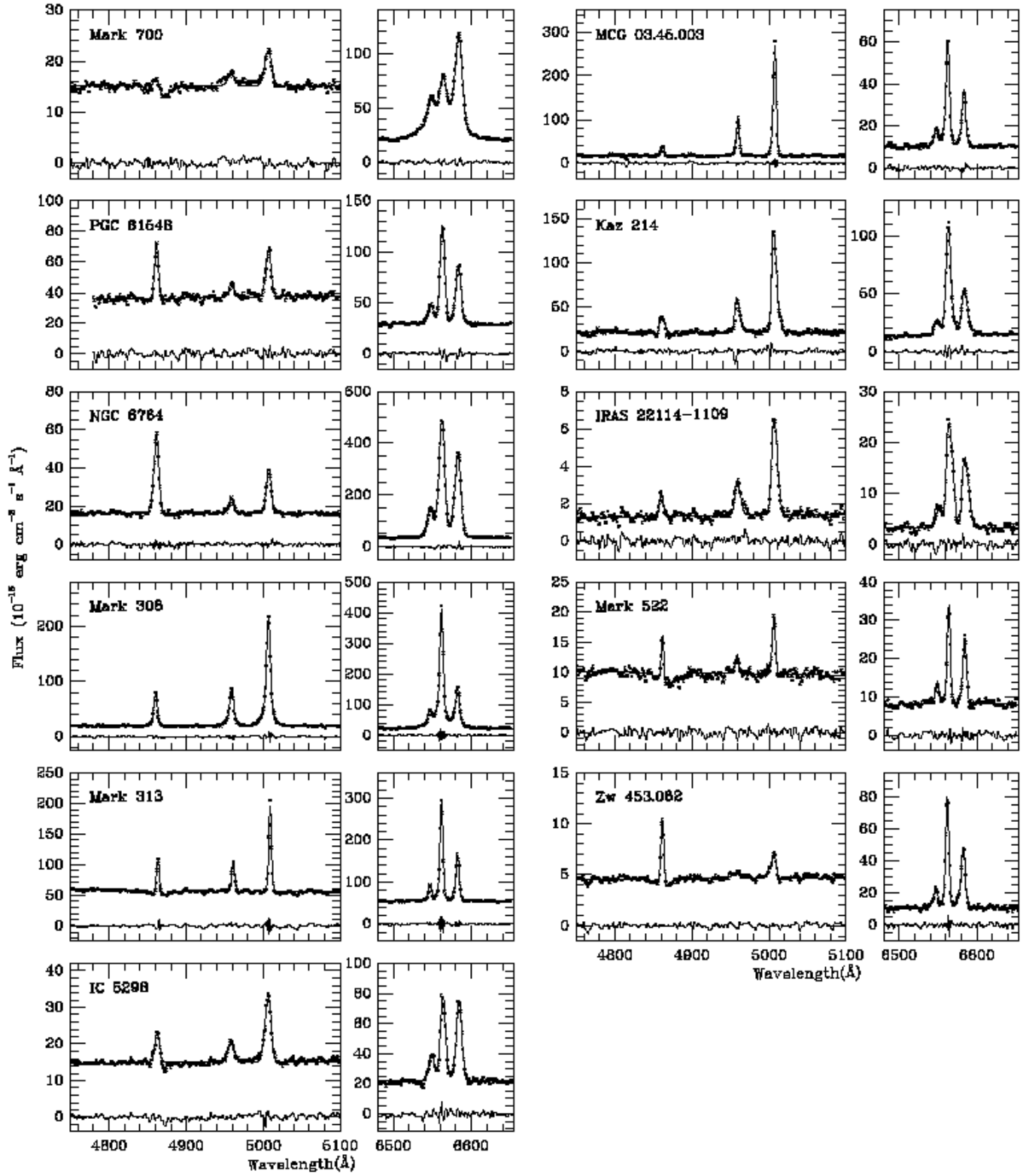
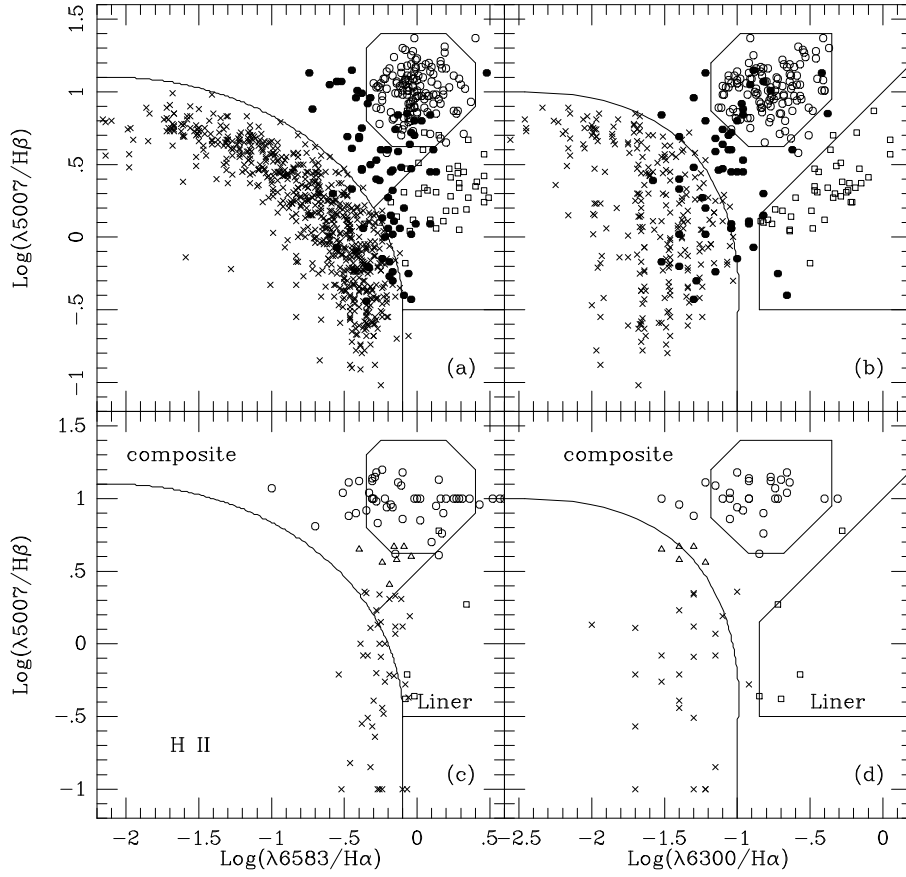


Fig. 1. Blue and red spectra for the 53 galaxies studied in this paper (end).



**Fig. 4.** Diagnostic diagrams showing the  $\log(\lambda 5007 / \text{H}\beta)$  vs.  $\log(\lambda 6583 / \text{H}\alpha)$  – boxes (a) and (c) – and  $\log(\lambda 5007 / \text{H}\beta)$  vs.  $\log(\lambda 6300 / \text{H}\alpha)$  – boxes (b) and (d). H II regions are represented by crosses, Seyfert 2 galaxies by open circles, and Liners by open squares. In (a) and (b), filled circles represent “transition objects”, i.e. objects which, in at least one of the diagrams, fall outside the arbitrarily delimited regions assigned to H II regions, Seyfert 2s and Liners. In (c) and (d) we plotted the individual components. The symbols are the same as in the upper panels; open triangles represent objects which could not be classified (“?” in Table 6).